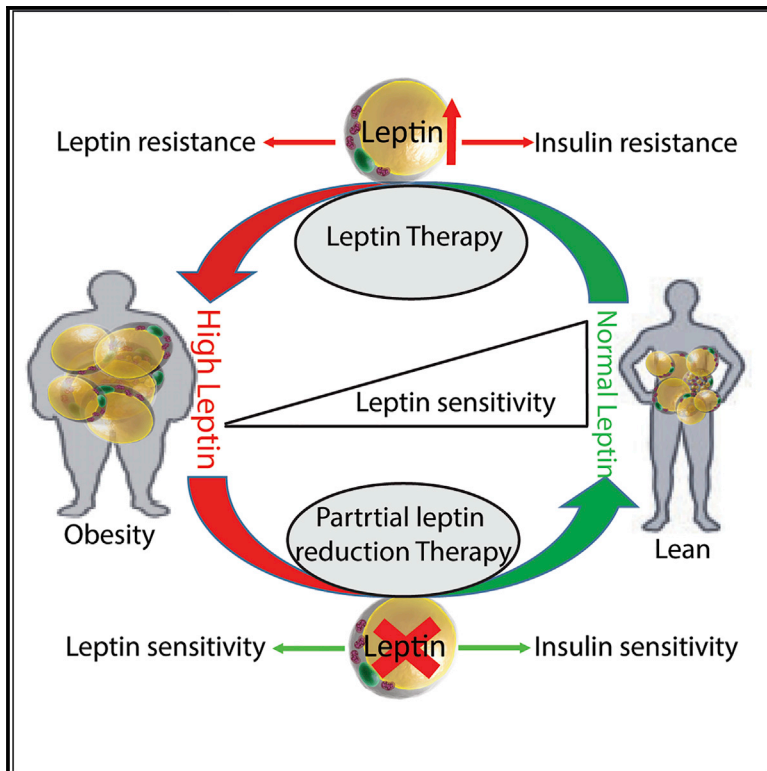# Partial Leptin Reduction as an Insulin Sensitization and Weight Loss Strategy

Graphical Abstract

Authors

Shangang Zhao, Yi Zhu,
Robbie D. Schultz, ...,
Kevin W. Williams, Zhiqiang An,
Philipp E. Scherer

Correspondence

philipp.scherer@utsouthwestern.edu

In Brief

Zhao et al. show that in the context of obesity, partial leptin reduction restores hypothalamic leptin sensitivity and leads to reduced food intake, increased energy expenditure, and improved insulin sensitivity. Thus, strategies aimed at partially reducing circulating leptin may represent a promising approach for the treatment of obesity and diabetes.

Highlights

- Hyperleptinemia is a driving force for obesity and its associated metabolic syndrome

- Partial reduction of leptin protects mice from diet-induced obesity

- Treatment of obese mice with a leptin neutralizing antibody reduces food intake

- Partial leptin reduction restores leptin sensitivity in hypothalamic neurons

Partial Leptin Reduction as an Insulin Sensitization and Weight Loss Strategy

Shangang Zhao,[1] Yi Zhu,[1] Robbie D. Schultz,[2] Na Li,[1,3] Zhenyan He,[4,5] Zhuzhen Zhang,[1] Alexandre Caron,[4] Qingzhang Zhu,[1] Kai Sun,[1,6] Wei Xiong,[2] Hui Deng,[2] Jia Sun,[4,5] Yingfeng Deng,[1] Min Kim,[1,7] Charlotte E. Lee,[4] Ruth Gordillo,[1] Tiemin Liu,[4] Angela K. Odle,[8] Gwen V. Childs,[8] Ningyan Zhang,[2] Christine M. Kusminski,[1] Joel K. Elmquist,[4] Kevin W. Williams,[4] Zhiqiang An,[2] and Philipp E. Scherer[1,9,*]

[1]Touchstone Diabetes Center, Department of Internal Medicine, The University of Texas Southwestern Medical Center, Dallas, TX, USA
[2]Texas Therapeutics Institute, Brown Foundation Institute of Molecular Medicine, The University of Texas Health Science Center at Houston, Houston, TX, USA
[3]Department of Endocrinology and Metabolism, Tianjin Medical University General Hospital, Tianjin 300052, China
[4]Division of Hypothalamic Research, Department of Internal Medicine, The University of Texas Southwestern Medical Center, Dallas, TX, USA
[5]Department of Neurosurgery and Endocrinology, Zhujiang Hospital, Southern Medical University, Guangzhou 510282, China
[6]Center for Metabolic and Degenerative Diseases, Brown Foundation Institute of Molecular Medicine, The University of Texas Health Science Center at Houston, Houston, TX, USA
[7]Department of Biological Sciences, School of Life Sciences, Ulsan National Institute of Science and Technology, Ulsan, South Korea
[8]Neurobiology & Developmental Sciences, College of Medicine, University of Arkansas for Medical Sciences
[9]Lead Contact
*Correspondence: philipp.scherer@utsouthwestern.edu
https://doi.org/10.1016/j.cmet.2019.08.005

SUMMARY

The physiological role of leptin is thought to be a driving force to reduce food intake and increase energy expenditure. However, leptin therapies in the clinic have failed to effectively treat obesity, predominantly due to a phenomenon referred to as leptin resistance. The mechanisms linking obesity and the associated leptin resistance remain largely unclear. With various mouse models and a leptin neutralizing antibody, we demonstrated that hyperleptinemia is a driving force for metabolic disorders. A partial reduction of plasma leptin levels in the context of obesity restores hypothalamic leptin sensitivity and effectively reduces weight gain and enhances insulin sensitivity. These results highlight that a partial reduction in plasma leptin levels leads to improved leptin sensitivity, while pointing to a new avenue for therapeutic interventions in the treatment of obesity and its associated comorbidities.

INTRODUCTION

Obesity remains one of the most prominent risk factors for a large number of chronic diseases, including diabetes, cardiovascular disease, fatty liver disease, and most types of cancer (Scherer, 2016). Despite lifestyle and surgical interventions, and some limited pharmacological therapies, there remains an unmet need to promote and sustain significant weight loss in overweight and obese individuals (Kusminski et al., 2016). The inefficacy of homeostatic weight control in the context of obesity remains one of the largest global public health issues.

As one of the first adipokines identified, hopes were extremely high that leptin could reduce food intake and promote energy expenditure (Friedman and Halaas, 1998). Congenital loss of leptin results in severe obesity in both rodents and humans (Montague et al., 1997). Administration of recombinant leptin provides an effective means to reduce obesity in leptin-deficient individuals (Farooqi et al., 1999). Furthermore, extremely low levels of leptin, evident in lipodystrophic patients, can be corrected using exogenous leptin treatment, which dramatically improves lipid and carbohydrate metabolism (Shimomura et al.,

Context and Significance

The hormone leptin is believed to reduce feeding and thus has been tested in the clinic as a treatment for obesity. However, this approach has mostly failed for most patients, suggesting that common forms of obesity are associated with a state of leptin resistance. Surprisingly, Phil Scherer and his colleagues find that in mice with diet-induced obesity, a partial reduction of circulating leptin either by genetic approaches or by a leptin neutralizing antibody restores sensitivity of the body to the remaining circulating leptin, resulting in weight loss and improvements in diabetes. Thus, the team proposes a major conceptual shift to the treatment of obesity; namely, rather than treating obese individuals with exogenous leptin, the appropriate approach would be to induce a partial reduction in endogenous circulating leptin by treatment with a leptin neutralizing antibody. This avenue might constitute a promising anti-obesity and anti-diabetic clinical therapy in the near future.

1999). However, injecting additional leptin, in the context of conventional obesity, is largely ineffective. Obese individuals do not lack leptin; rather, they display higher circulating levels of leptin, and these elevated levels are associated with leptin resistance and impaired leptin signaling in the brain (Zelissen et al., 2005). Leptin "resistance" is therefore defined as the inability of elevated leptin levels (either endogenous or pharmacologically administered) to reduce food intake and cause weight loss (Ahima and Flier, 2000; Flier and Maratos-Flier, 2017; Friedman, 2016). However, there is also the concept of "selective leptin resistance" (Mark, 2013), whereby not all leptin signaling pathways are equally affected. While the complete lack of leptin signaling can cause infertility, not all obese individuals are infertile since some leptin signaling is preserved both centrally and peripherally (Hausman et al., 2012).

Hyperleptinemia is necessary and sufficient to induce leptin resistance in wild-type (WT) mice (Knight et al., 2010), as well as in leptin super-sensitive *ob/ob* mice upon chronic leptin injection (Koch et al., 2014). In contrast, congenital elevation of leptin leading to a "transgenic skinny" mouse resulted in increased glucose metabolism and insulin sensitivity (Ogawa et al., 2002). Similarly, chronic infusions of leptin intracerebroventricularly at doses of 3 ng/h or greater resulted in complete depletion of visible adipose tissue, which was maintained throughout 30 days of continuous intracerebroventricular infusion (Halaas et al., 1997). Thus, the mechanisms of leptin resistance are still poorly understood (Flier and Maratos-Flier, 2017).

Developmentally, leptin plays a critical role in the generation of the neuronal circuitry (Pinto et al., 2004; Bouret et al., 2004; Zeltser, 2015). While the congenital loss of leptin results in severe obesity, to date, no attempts have been made to achieve a *reduction* in leptin levels only in the adult stage, while leaving the remaining adipose tissue depots intact and functional.

Here, based on two distinct genetic approaches and a third independent antibody-based approach, we report a series of novel and unique observations, in which a *decremental reduction* in circulating leptin levels in adult obese mice initiates an unexpected and significant improvement in several parameters of energy balance and glucose homeostasis. This system-wide response includes significant weight loss, reduced food intake, and increased energy expenditure, all consistent with enhanced leptin sensitization.

RESULTS

Increasing Leptin Levels in Obese Mice Enhances Body Weight Gain

Leptin gene expression and circulating leptin levels are tightly regulated under most physiological conditions. Here, we show that acute high-fat diet (HFD) feeding of WT mice significantly upregulates leptin expression in gonadal white adipose tissue (gWAT), with a lesser induction evident for subcutaneous white adipose tissue (sWAT) and brown adipose tissue (BAT) (Figure 1A). Consistent with these observations, a higher circulating leptin level is observed in mice exposed to short-term HFD feeding, suggesting that the gonadal fat pad is a major contributor to circulating leptin levels (Figure 1B).

To further define the physiological roles of leptin, we generated an inducible adipocyte-specific leptin transgenic mouse

(ALep-TG). We fed lean ALep-TG and littermate control (Ctrl) mice with chow diet supplemented with Dox600 (600 mg/kg Dox) for 1 week and observed that leptin expression is significantly induced in sWAT, gWAT, and BAT depots, with no induction evident in the liver in ALep-TG mice compared to control mice (Figure S2A). Importantly, no significant differences were observed for adiponectin and other key genes (such as TNFα and ATGL) in the different fat depots with acute leptin induction, confirming that our transgenic mouse model is specific to leptin (Figures S2B–S2D). Upon Dox supplementation in mice on chow diet, the circulating levels of leptin are much higher in ALep-TG mice, by approximately 3-fold compared to Ctrl mice (Figure S2E), without a significant change in adiponectin levels (Figure S2F).

To assess the role of leptin in the context of obesity, ALep-TG and Ctrl mice were fed an HFD for 6 weeks to induce obesity and leptin resistance. Prior to induction, circulating levels of leptin per total fat mass are similar between Ctrl and Alep-TG groups (Figure 1C). Transgenic leptin was then induced by adding DOX600 to the HFD to both groups. Following induction with DOX for 6 weeks, ALep-TG mice display significantly higher circulating leptin levels within the physiological range, compared to Ctrl mice (Figure 1C). Interestingly, in parallel with this increase in leptin, insulin levels are also doubled (Figure 1D) and adiponectin levels are lower compared to Ctrl mice (Figure 1E). Prior to leptin gene induction, there is no difference in body weight and glucose tolerance between Ctrl and ALep-TG mice (Figures 1F and 1I). Upon transgene induction with Dox, we observe that the higher leptin levels in Alep-TG trigger accelerated body weight gain (Figure 1F) with significant increases in fat mass (Figure 1G), but not in lean mass (Figure 1H), concomitant with impaired glucose tolerance and insulin sensitivity (Figures 1J and 1K). Of note, upon switching the diet from HFD only to HFD with DOX600, both ALep-TG and Ctrl mice reduce their rate of body weight gain. This may be due to a slight reduction in food intake upon exposure to the new diet. Since both ALep-TG and Ctrl mice were exposed to the exact same diet all the times, this does not affect the interpretation of the results observed. Compared to Ctrl mice, ALep-TG mice display enhanced hepatic steatosis with an associated "whitening" of BAT; the latter frequently associates with a reduction in brown fat function (Kusminski et al., 2014; Zhu et al., 2016) (Figures 1L and 1M). Taken together, these results suggest that solely increasing the leptin levels in the obese state, without altering adipose tissue in any other way during the onset of the leptin increase, greatly exacerbates metabolic dysfunction. This supports the notion that enhancing leptin levels per se in the obese state is sufficient to trigger pathological changes.

A Cas9-CRISPR-Based Approach for Inducible Elimination of Leptin Specifically from the Mature Adipocyte

In light of the fact that high leptin is sufficient to induce leptin resistance and trigger pathological changes, we wondered what would occur if leptin levels were reduced in the setting of obesity at the adult stage. In order to do this, we generated Cas9-sgLeptin mice, a strain that enables us to do a doxycycline-inducible elimination of leptin in the adipose tissues of adult mice. As expected, within as little as 2 days of Dox-HFD feeding,
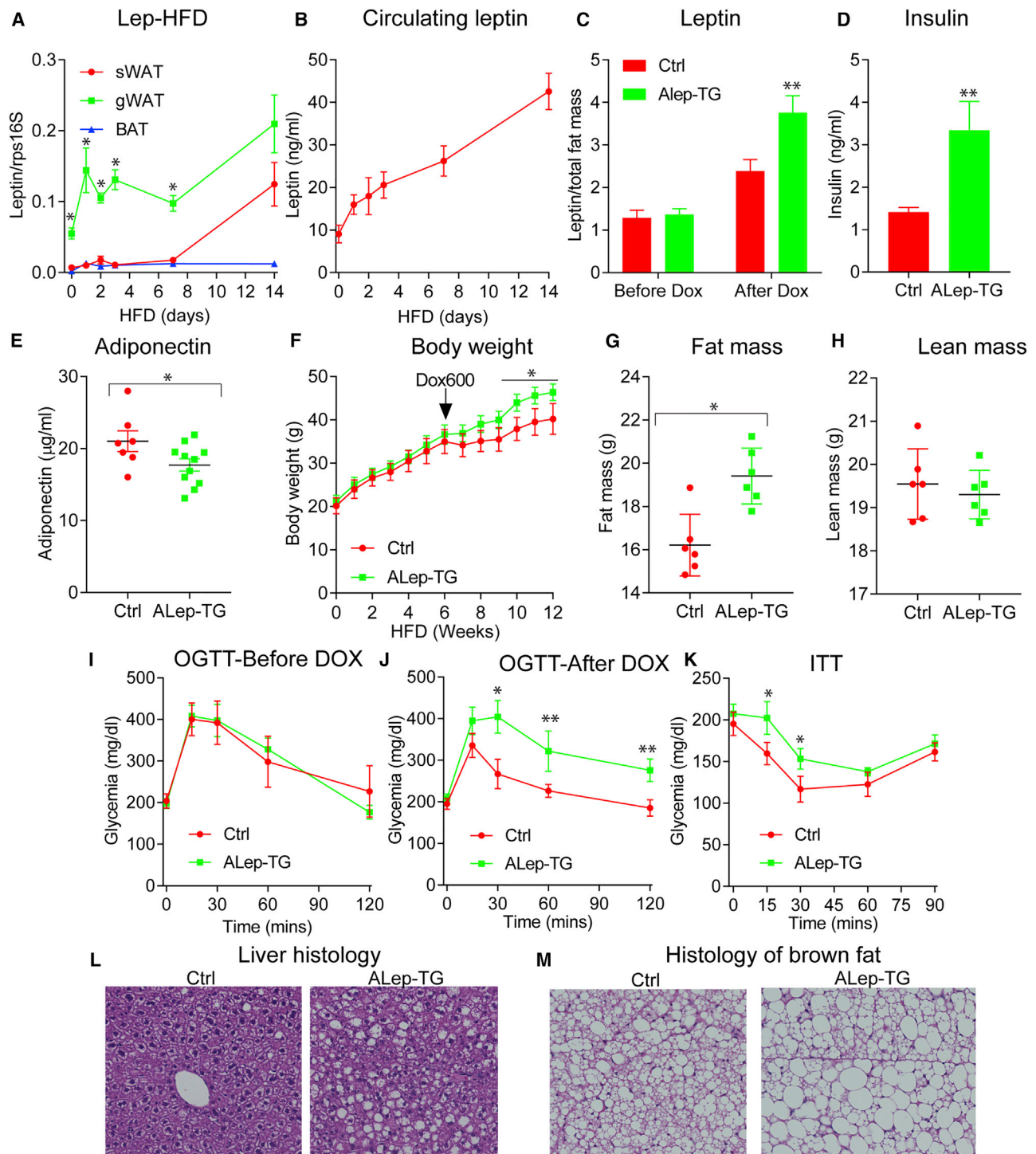
Figure 1. Increasing Leptin Levels in Obese Mice Exacerbates Obesity and Metabolic Dysfunction

(A) Leptin gene expression in various fat depots collected from wild-type (WT) mice (n = 5 per time point) transferred from a chow diet to an HFD.

(B) Circulating leptin levels in WT mice (n = 10) from chow diet to HFD; ALep-TG (n = 10) and littermate control (n = 11) mice at 8 weeks of age were placed on HFD for 6 weeks and then switched to HFD diet with Dox (600 mg/kg).

(C–M) Leptin (C), insulin (D), and adiponectin (E) levels were measured before and after supplementing DOX in the diet, and leptin levels were normalized to total fat mass. Body weight gain (F), fat mass (G), lean mass (H), oral glucose tolerance tests (OGTTs) before (I) and after (J) DOX diet as well as insulin tolerance tests (ITTs) (K) after DOX were done in ALep-TG and littermate Ctrl mice. Histological analyses with H&E stain of livers (L) and brown fat (M) were assessed. Data are given as mean ± SEM. Error bars indicate SEM. *p < 0.05; **p < 0.01; ***p < 0.001.
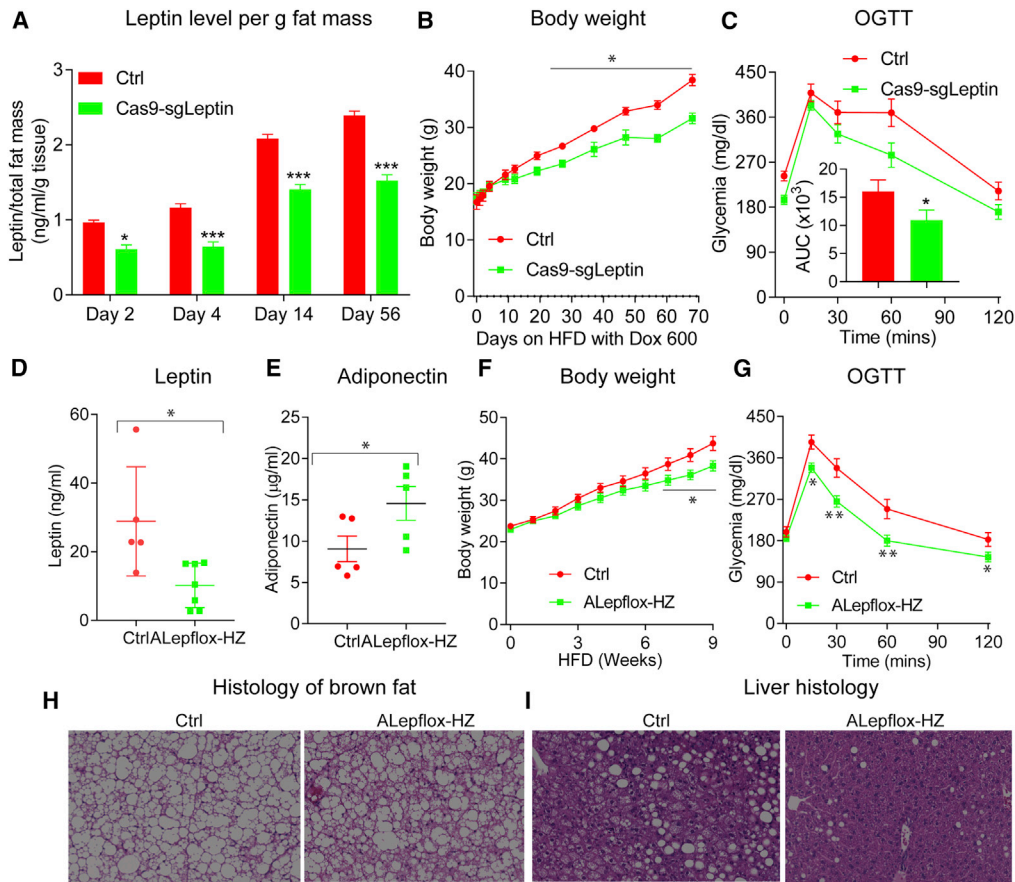
Figure 2. Partial Leptin Reduction in Mice Protects against Diet-Induced Obesity
Cas9-sgLeptin and littermate control mice at 8 weeks of age were placed on HFD with Dox 600 for 10 weeks.
(A) Circulating leptin levels per total fat mass in Cas9-sgLeptin (n = 5) and littermate control mice (n = 5) at the indicated time points.
(B) Body weight gain during HFD feeding in Cas9-sgLeptin (n = 10) and littermate control mice (n = 10).
(C) OGTTs on Cas9-sgLeptin (n = 10) and control mice (n = 10). Area under the curve (AUC) was calculated and inserted inside this figure; ALepflox-HZ and littermate control mice at 8 weeks of age were placed on HFD with Dox 600 for 9 weeks. Two different cohorts of mice were used in this study.
(D and E) Circulating leptin (D) and adiponectin (E) levels measured in the first cohort of ALepflox-HZ (n = 7) and control mice (n = 5).
(F) Body weight gain in ALepflox-HZ (n = 12) and control mice (n = 10).
(G) OGTT in ALepflox-HZ (n = 12) and Ctrl mice (n = 10).
(H and I) After euthanizing the mice, brown fat (H) and liver (I) were processed for H&E staining.
Data are given as mean ± SEM. Error bars indicate SEM. *$p < 0.05$; **$p < 0.01$; ***$p < 0.001$.

Cas9-sgLeptin mice exhibit a much lower circulating leptin levels per total fat mass (Figure 2A), and this leptin reduction is well maintained throughout the experiment and still reduced at 8 weeks (Figure 2A). Remarkably, compared to littermate Ctrl mice, Cas9-sgLeptin mice display a significant reduction in body weight gain (Figure 2B). This is an entirely unexpected finding since we assumed that a reduction in leptin would prompt increased weight gain, as typically observed with a congenital leptin deficiency in the *ob/ob* mouse (Nunziata et al., 2019). The measurements of plasma leptin concentrations, however, show that the system is not particularly effective since the circulating levels of leptin are reduced by less than 50%, when compared with Dox-treated littermate Ctrl mice (Figure 2A). We consistently observed the association between lowering leptin and reduced body weight gain over multiple cohorts, along with improvements in oral glucose tolerance (Figure 2C). However, since this response was unexpected and in direct contrast

to the prior observations made using heterozygous *ob+* mice, we decided to validate the observed effects with additional independent approaches.

Genetic Elimination of Leptin in the Adult Mouse Using a Classical Cre-loxP System

To confirm these observations, we employed a classical Cre-loxP approach for leptin elimination. In order to achieve a situation similar to the Cas9-CRISPR-based approach and also to be able to compare the phenotype with the heterozygous *ob+* mice, in which partial leptin deficiency favors diet-induced obesity and unfavorable metabolic phenotypes (Begriche et al., 2008), we began utilizing ALepflox-HZ mice, in which we eliminate only one copy of the leptin gene at the adult stage. As expected, compared to littermate Ctrl mice, the circulating levels of leptin levels are reduced by approximately 50% in ALepflox-HZ mice (Figure 2D), proportional to
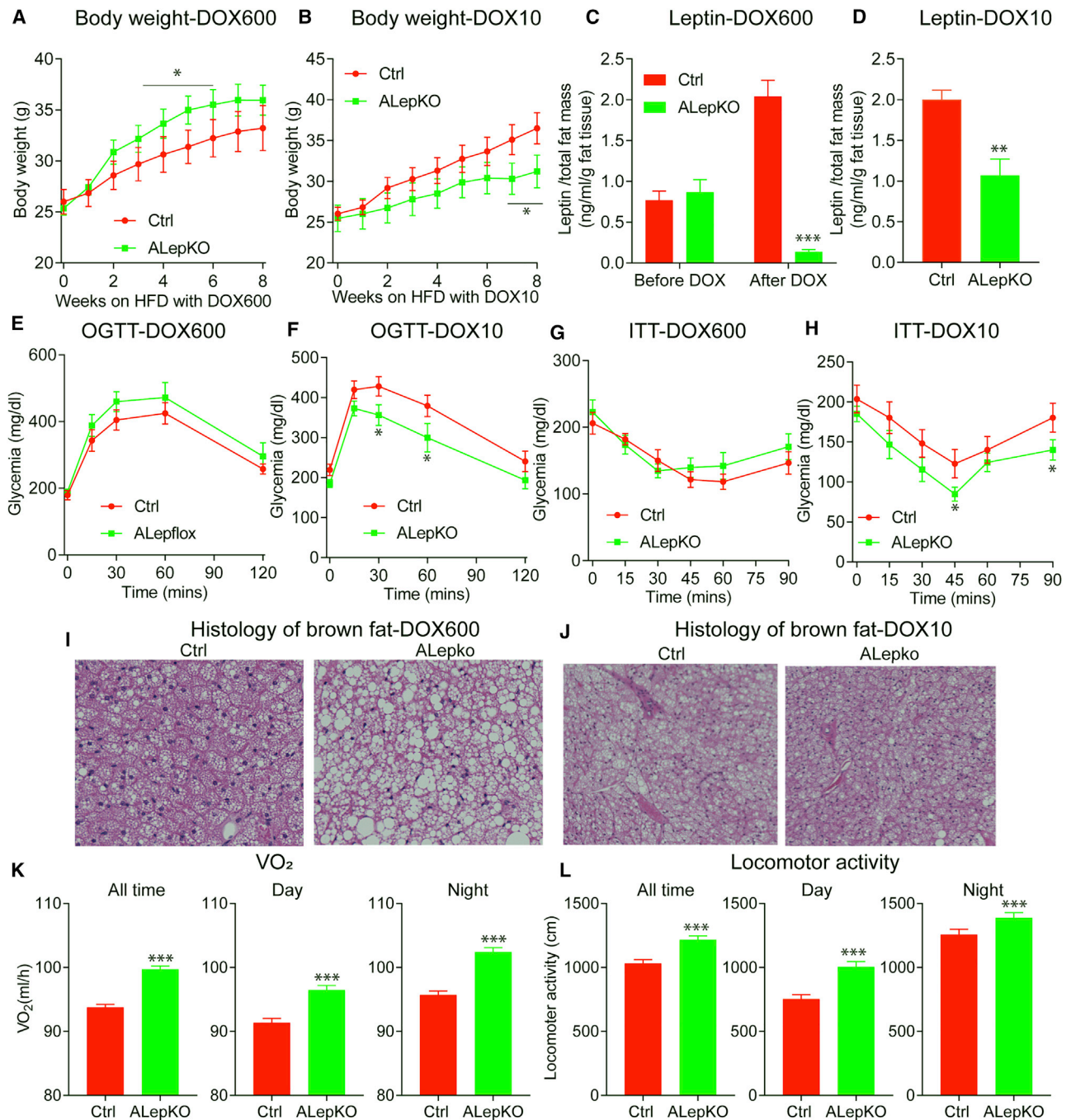
Figure 3. Partial, Not Complete, Reduction of Circulating Leptin Protects Mice from Obesity

ALepKO and littermate control mice were placed on HFD supplemented with two different amounts of doxycycline (DOX) (600 mg/kg [DOX600] and 10 mg/kg [DOX10]). Body weights, circulating leptin levels, OGTTs, ITTs, and histological analysis were performed.

(A) Body weight gain of ALepKO (n = 6) and littermate controls (n = 7) on DOX600.

(B) Body weight gain ALepKO (n = 7) and littermate controls (n = 7) on DOX10.

(C) Circulating leptin levels per total fat mass of ALepKO (n = 7) and littermate controls (n = 6) before and after DOX 600.

(D) Circulating leptin levels per total fat mass of ALepKO (n = 9) and littermate controls (n = 8) on DOX10.

(E) OGTT on ALepKO (n = 8) and littermate controls (n = 6) on DOX600.

(F) OGTTs on ALepKO (n = 6) and littermate controls (n = 11) on DOX10.

(G) ITTs on ALepKO (n = 6) and littermate controls (n = 6) DOX600.

(H) ITTs on ALepKO (n = 6) and littermate controls (n = 8) on DOX 10.

(I) Brown adipose tissue histology on DOX600.

the effects of eliminating 50% of the gene dosage. ALepflox-HZ mice display an increase in circulating adiponectin levels after 8 weeks of HFD (Figure 2E). In line with our previous observations, in comparison to littermate Ctrl mice, following Dox-HFD feeding, ALepflox-HZ mice display a significant reduction in body weight gain, concomitant with a significant improvement in glucose tolerance (Figures 2F and 2G). Of particular note, ALepflox-HZ mice do not display the conventional "whitening" of brown fat (Figure 2H) and display a reversal in HFD-induced hepatic steatosis (Figure 2I). Our data, thus, fully support the observations made using Cas9-sgLeptin mice and lead us to propose that a *partial reduction* of plasma leptin levels in the adult stage is beneficial in the context of obesity.

In the absence of leptin resistance, leptin effectively reduces food intake and increases energy expenditure (Friedman, 2016). Eight-week-old, young, and lean chow-fed mice maintain high levels of leptin sensitivity. As such, reducing leptin levels in lean chow-fed mice could serve as a valid model to verify our ALepKO mice, a mouse model in which we delete two copies of the leptin gene. We therefore utilized chow diet containing the standard dose of DOX600 (600 mg/kg) to induce *complete* leptin gene deletion and observed that the circulating levels of leptin were greatly reduced by more than 90% (Figure S3A). As expected, under these conditions of high leptin sensitivity at baseline with Dox-chow feeding, reducing leptin levels in ALepKO mice results in accelerated body weight gain, with associated worsened glucose tolerance and reduced insulin sensitivity (Figures S3B–S3D). As such, this mouse model follows the "classical" model, whereby maximal leptin sensitivity is present and reducing leptin triggers further lowering of leptin signaling centrally.

We then performed a more detailed set of experiments on HFD-fed animals. We used two different concentrations of DOX in HFD that we anticipated would allow us to go from near complete elimination of leptin to a partial reduction in leptin. The high dose of DOX600-HFD feeding (600 mg/kg Dox) triggers a rapid and significant increase in body weight gain over the 6-week period following initiation of leptin gene disruption (Figure 3A). Conversely, at a much lower dose (DOX10), we observe a significant *reduction* in body weight gain over the course of a 6-week follow-up period (Figure 3B). Prior to DOX induction, ALepKO and littermate Ctrl mice show similar leptin levels (Figure 3C). After DOX induction, the two different doses of Dox achieve a dose-dependent proportional reduction in plasma leptin levels in ALepKO mice (Figures 3C and 3D). It is interesting to note that ALepKO mice on HFD-DOX600 rapidly increased body weight within the first 3 weeks, followed by a reduction in body weight gain over the next 5 weeks. This is in stark contrast to classical *ob/ob* mice and can be explained at least in part by the remaining 10% leptin in circulation. Consistent with the body weight phenotype, in comparison to Ctrl mice, ALepKO mice on DOX600 display no difference in glucose tolerance, slightly reduced insulin sensitivity, and whitened brown fat (Figures 3E, 3G, and 3I). In contrast, ALepKO mice on a

DOX10 diet show beneficial effects on glucose metabolism and insulin sensitivity, with a reduction in the degree of "whitened" brown fat (Figures 3F, 3H, and 3J). The latter represents a phenotype similar to what we observe for our ALepflox-HZ mice during high-dose Dox-HFD (600 mg/kg Dox) feeding (Figures 2E and 2F). Collectively, this further underlines the point that a *partial reduction*, not a *complete elimination*, of leptin yields a completely unexpected, unique, and previously undescribed body weight phenotype.

In order to elucidate the possible mechanism of this unique body weight phenotype relying on a partial reduction of leptin, ALepKO mice fed DOX10-HFD were placed in metabolic cages. Following partial leptin reduction, compared to Ctrl mice, ALepKO mice increase their oxygen consumption rates, both during the light and dark cycles over 5 days of recording (Figures 3K and S3E). In addition, locomotor activity is significantly increased in ALepKO mice during both cycles (Figures 3L and S3F). Finally, a moderate decrease in the respiratory exchange ratio (RER) is apparent during the dark cycle (Figure S3G), reflecting a shift toward free fatty acids as a major energy source. However, the changes in the RER, in addition to other metabolic cage parameters, do not reach statistical significance (Figures 3G and 3H). In addition, increased UCP-1 and PGC1-α were observed in sWAT and brown fat. Collectively, these results suggest that mice with a partial reduction in circulating levels of leptin display enhanced energy expenditure and locomotor activity, characteristic of a system with enhanced leptin sensitivity.

To further confirm our unique findings based on a partial leptin reduction, we first eliminated leptin gene expression in ALepKO mice by placing them on a chow diet containing the standard dose of DOX600 for 1 week. ALepKO mice were then switched to an HFD lacking DOX. By utilizing this strategy, we achieved approximately half of the circulating levels of leptin evident in control mice, measured after 8 weeks of HFD (Figure S3I). Although we appreciate that a portion of adipocytes will differentiate *de novo* under these conditions (and will carry WT copies of the leptin gene), these mice continue to display a *partial leptin reduction* (Ctrls at 40 ng/mL, ALepKOs at 19 ng/mL). Consistent with our previous findings, the ALepKO mice here also display a significant reduction in body weight gain, concomitant with a marked improvement in glucose tolerance, compared to littermate Ctrl mice (Figures 3J and 3K).

As obesity triggers high circulating levels of leptin and is closely associated with leptin resistance, it is of great interest to examine whether a partial leptin deletion in obese mice can *reverse* the obesity-associated metabolic syndrome, post hoc HFD-induced metabolic dysfunction. To achieve this, ALepKO and control mice were placed on HFD (without Dox) for 6 weeks. As expected, under baseline conditions, ALepKO and littermate Ctrl mice gain comparable body weight and display similar circulating levels of leptin (Figure S3M). Following 6 weeks of HFD feeding, mice were then switched to the low dose of Dox-HFD (10 mg/kg Dox) to initiate a partial reduction of leptin in ALepKO

(J) Brown adipose tissue histology on DOX10.
(K) Oxygen consumption (VO₂) of ALepKO (n = 6) and littermate controls (n = 6) on DOX10 in metabolic cages.
(L) Locomotor activity of ALepKO mice (n = 6) and littermate controls (n = 6) on DOX10 during the dark period, daytime, and across the entire 24-h period.
Data are given as mean ± SEM. Error bars indicate SEM. *p < 0.05; **p < 0.01; ***p < 0.001.

mice. Compared to littermate Ctrl mice, ALepKO mice display an approximately 50% reduction in plasma leptin levels (Figure S3L). Furthermore, ALepKO mice fail to further gain more body weight and exhibit greatly improved glucose tolerance (Figures 3M and 3N). Combined, these results further confirm that hyperleptinemia per se is a major driving force for metabolic dysfunction, and a partial reduction of circulating leptin levels can serve as an effective strategy to overcome obesity and associated metabolic dysfunction.

Neutralizing Leptin Antibodies Reduce the Extent of Weight Gain

Given that a partial reduction in the circulating levels of leptin in the context of obesity produces beneficial effects by improving glucose homeostasis, we began to produce neutralizing monoclonal antibodies against human leptin. We have generated a large number of different monoclonal preparations. Upon analysis of the data, three monoclonal antibodies (hLep2, hLep3, and hLep5) exhibit leptin neutralizing activity *in vitro* and were selected for further *in vivo* studies (Figure 4A).

We treated a cohort of obese mice (n = 5 per group), either with vehicle or the three neutralizing antibodies. As shown in Figure S4B, vehicle-treated mice exhibit a gradual increase in body weight, while mice treated with the three neutralizing antibodies display various levels of reduced body weight gain. hLep3 displays the most potent effects. In addition, none of the mice show differences in glucose tolerance prior to treatment (Figure S4C). Following 2 weeks of antibody treatment, hLep3- and Lep5-treated mice show enhanced glucose tolerance, concomitant with a profound reduction in gonadal fat pad weight, while hLep2-treated mice show no or little effect (Figures S4C and S4D). Based on this initial characterization, the hLep3-neutralizing antibody was selected for further experimental studies.

In order to rule out possible endotoxin-induced weight loss, we performed a similar study on obese mice with an isotype control antibody, a human IgG1 monoclonal antibody that we identified in house against human cytomegalovirus (hCMV virus). We generated and purified control antibodies and hLep3 antibodies with identical procedures. After 2 weeks of treatment, in comparison to isotype control antibody-treated mice, hLep3-treated mice significantly reduced body weight gain (Figures 4A and 4B) and food intake (Figure 4C). In addition, before antibody injection, there were no differences in glucose tolerance and total fat mass (Figures 4D and 4F). hLep3 treatment greatly increased glucose tolerance (Figure 4E) and significantly reduced fat mass (Figure 4F). These results indicate that the beneficial effects are indeed directly related to the activity of the leptin neutralizing antibodies.

To gain further insights into the possible causes underlying the beneficial effects, vehicle- or hLep3-treated mice were placed in metabolic cages. Following hLep3 treatment, we achieved a 50% reduction in circulating free leptin levels (Figure S4F). As a consequence, hLep3-treated mice reduce food intake (Figure 4G) and show a significant reduction in the RER (Figure 4H), without any significant differences in locomotor activity (Figures S4K and S4L).

HFD feeding typically affects brown fat in a negative manner, which results in a high degree of "whitened" BAT. This deterioration in BAT quality and function was prevented (in fact

reversed) with hLep3 antibody treatment (Figure 4I). Consistent with the histology, the gene expression levels of thermogenic genes, such as *Ucp1* and *Pgc1α*, are significantly upregulated in sWAT and BAT of hLep3 antibody-treated mice (Figures S4G and S4H). With regard to the liver, we observe a marked reduction in diet-induced hepatic steatosis following hLep3 antibody treatment (Figure 4J). In adipose tissue itself, hLep3 treatment reduces the degree of adipose tissue inflammation and reduces the average adipocyte size (Figures S4I and S4J). Taken together, these results support our hypothesis that a partial reduction in the circulating levels of leptin, through the use of neutralizing antibodies, leads to a reduction in food intake and a re-activation of the thermogenic program in brown fat. Collectively, these responses to antibody treatment are consistent with a model of restored leptin sensitivity.

In order to deconvolute the relative contribution of food intake and non-shivering thermogenesis in the context of body weight reduction, we treated obese WT mice with vehicle or hLep3 antibody under thermoneutral conditions (to minimize the effects of non-shivering thermogenesis). Upon thermoneutral housing, hLep3-treated obese mice effectively reduce their body weight gain and preserve their glucose tolerance (Figure 4K), even in the absence of any notable brown fat activity (Figures S4M and S4N). Thermoneutral housing is a strong additive factor to further promote liver steatosis and fibrosis during HFD feeding. Surprisingly, hLep3 treatment of mice effectively reversed diet-induced hepatic steatosis, as evident by reduced hepatic lipid droplet accumulation, even under these thermoneutral conditions (Figure S4O). Taken together, our results indicate that the neutralizing leptin antibodies retain their full beneficial effects even under thermoneutral conditions. Moreover, it is predominantly the reduction in food intake that contributes toward the observed unique body weight phenotype. As an additional control, we administered Lep3 mAb and vehicle in *ob/ob* mice that do not have functional leptin. The Lep3 mAb shows no effect on weight gain and lacks any efficacy in *ob/ob* mice compared to WT control mice (Figure 4L). These results further demonstrate that hLep3 antibody functions exclusively on the basis of a reduction in systemic leptin levels.

Partial Leptin Deficiency in Obese Mice Reverses Leptin Resistance

The data so far indicate that a partial reduction in leptin leads to reduced food intake and enhanced adaptive thermogenesis, which is consistent with an enhanced degree of leptin sensitivity. As such, this prompted us to search for further evidence to support the concept of "restored" leptin sensitivity in obese mice. To this end, we first examined leptin sensitivity in leptin transgenic mice. As observed in Figures S5A and S5B, the expression of *Pomc* and *Agrp* in the mediobasal hypothalamus (MBH) region of the brain is significantly reduced in Alep-TG mice, compared with control mice. In contrast, the gene expression levels of *Socs3*, *Tnfα*, and interleukin-1β are significantly increased, indicative of a higher degree of leptin resistance associated with hypothalamic inflammation (Figures S5C–S5F).

In contrast to Alep-TG mice, a partial reduction in leptin, as achieved through genetic deletion or by utilizing neutralizing antibodies, leads to improvements in the MBH region of the brain, as reflected by increased *Pomc* expression and decreased
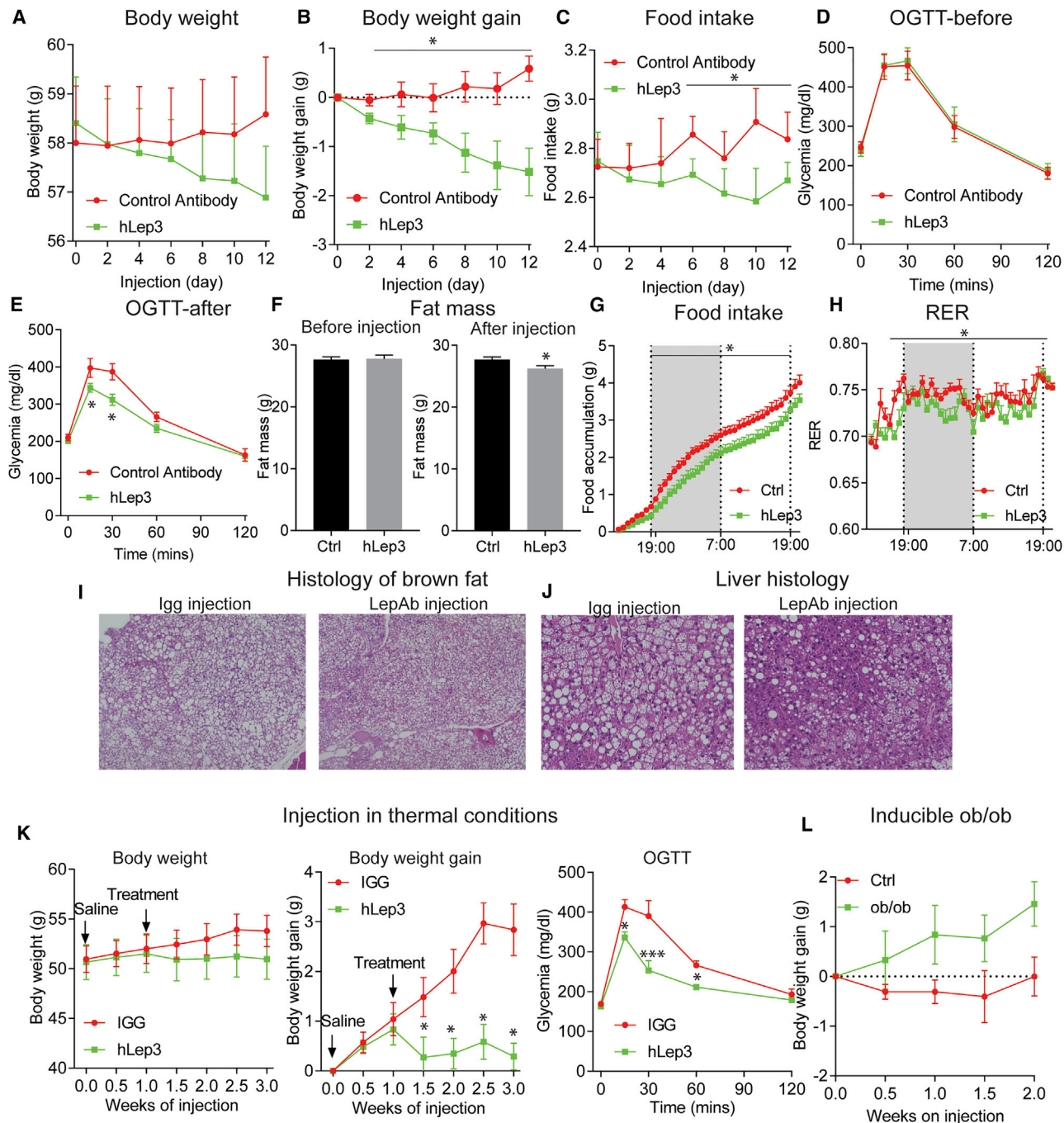
Figure 4. Decreasing Leptin Levels with Neutralizing Anti-leptin Antibodies Reduces Body Weight Gain and Liver Steatosis

(A–F) A cohort of obese mice (n = 8 per group) were treated either with control antibody or leptin neutralizing antibody (hLep3) for 2 weeks. Antibody injections were done every other day. Body weight (A) and food intake (C) were measured before each injection. Body weight gain was calculated (B), OGTTs were performed before (D) and after (E) antibody injection, and total fat mass (F) was measured by Eco-MRI. For the metabolic cage studies, obese WT mice (n = 6 per group) were treated with a control antibody (hIGG) or hLep3 antibody.

(G) Food consumption measured in metabolic cages after vehicle or hLep3 treatment.

(H) RER measured in vehicle- and hLep3-treated mice.

(I and J) After a 2-week treatment period, mice were euthanized, and brown fat and liver were collected for histology analysis. H&E staining of brown adipose tissue (I) and liver (J). Obese WT mice (n = 5 per group) were housed in thermoneutral chambers and treated with control antibody (hIGG) or hLep3 neutralizing antibody for 2 weeks.

(K) Effects of the neutralizing antibody hLep3 on body weight, body weight gain, and OGTTs on mice housed at thermoneutrality.

(L) Effect of hLep3 on body weight gain in inducible *ob/ob* mice.

Data are given as mean ± SEM. Error bars indicate SEM. $*p < 0.05$; $**p < 0.01$; $***p < 0.001$.
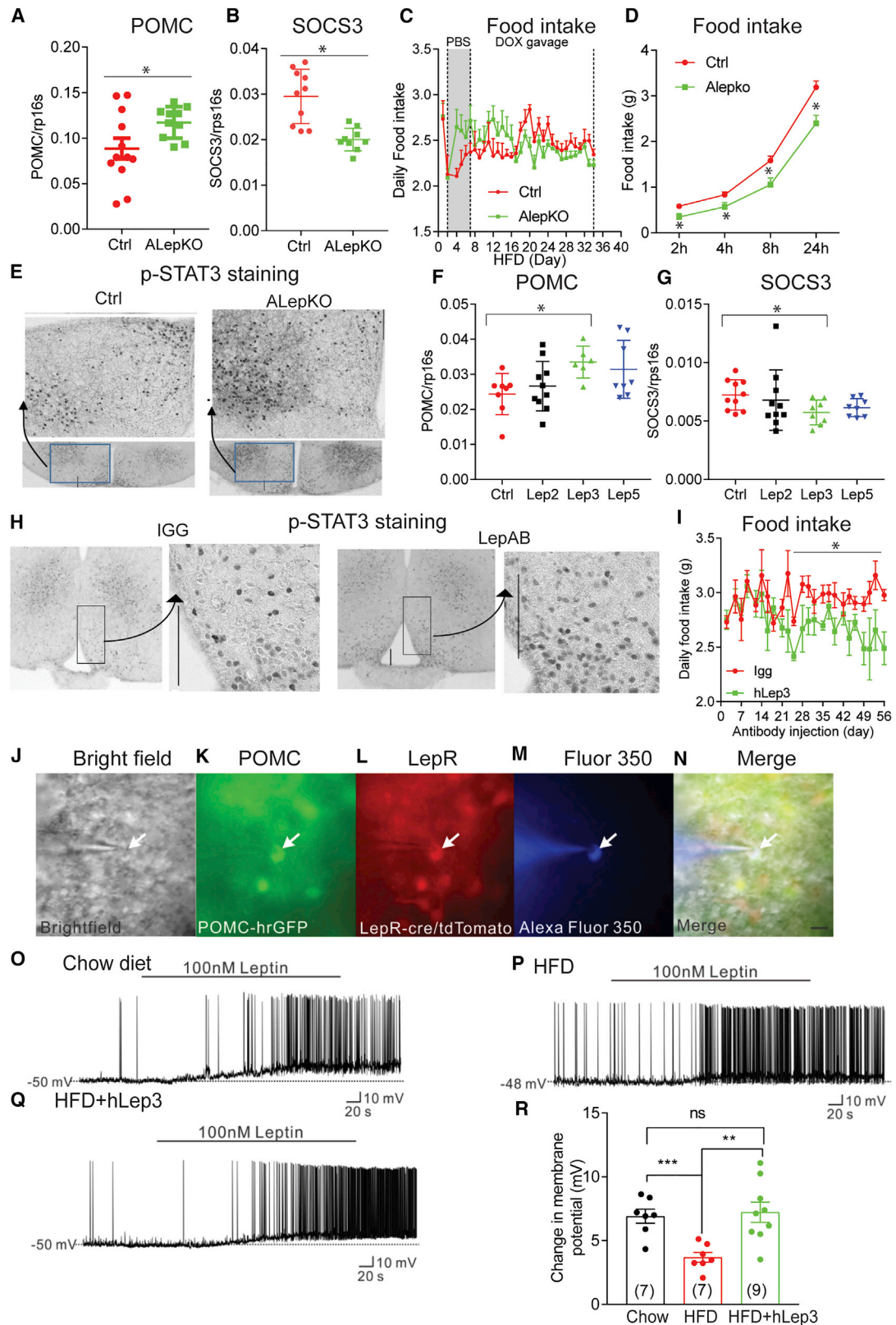
Figure 5. Leptin Sensitivity Is Inversely Correlated with Circulating Leptin Levels

(A and B) Expression of *pomc* (A) and *socs3* (B) in the ARH region of control (n = 12) and AlepKO mice (n = 12).

(C) Daily food intake was measured in control (n = 7) and ALepKO mice (n = 7) during PBS or a low-dose doxycycline (5 mg/kg body weight) oral gavage period.

Socs3 expression (Figures 5A, 5B, 5F, and 5G). Inflammation in the MBH region is ameliorated in ALepKO mice, as reflected by a reduction in *Tnfα* and interleukin-1β expression (Figures 5G and 5H). In line with these observations, following oral gavage of Dox at a dose of 5 mg/kg body weight to induce partial *ob* gene deletion, ALepKO mice exhibit a reduction in food intake, with evidently higher basal food intake than vehicle treatment (Figure 5C), consistent with enhanced leptin sensitivity. Moreover, following acute injection of leptin, ALepKO mice exhibit a greater reduction in food intake at multiple different time points (2, 4, 8, and 24 h) (Figure 5D), compared to littermate Ctrl mice. Interestingly, immunohistochemical staining reveals a marked increase in p-STAT3 in ALepKO mice or upon treatment of obese mice with neutralizing antibodies (Figures 5E and 5H). In addition, long-term treatment with neutralizing anti-mouse leptin antibodies (6 weeks) triggers a 10% reduction in food intake. Importantly, this reduction could be maintained for several weeks, without any loss of effectiveness of the treatment due to "desensitization" to the antibody (Figure 5I). This suggests that this approach could serve as an effective long-term weight loss strategy. In fact, genetic reduction of leptin levels in the adult mouse results in the maintenance of the effects reported for more than 10 months (Figure S5L), emphasizing that there is no "re-calibration" of homeostatic control of fat mass upon leptin reduction if the leptin reduction is performed in the adult animal.

In order to further confirm enhanced leptin sensitivity induced through reduction of leptin levels, we treated HFD-fed POMC-hrGFP::LepR-cre::tdtomato mice (Sun et al., 2016) with neutralizing leptin antibodies. POMC neurons were then targeted for whole-cell patch-clamp recordings, for which arcuate POMC neurons with or without the expression of leptin receptors could be identified (Figures 5J–5N). HFD feeding blunts the acute leptin-induced depolarization of leptin-receptor-expressing POMC neurons, when compared with chow-diet-fed mice (100 nM, chow diet fed, 7/10; change of resting membrane potential, 6.9 ± 0.6 mV; HFD fed, 7/12; change of resting membrane potential, 3.7 ± 0.4 mV, p < 0.001; Figures 5O and 5P). Importantly, leptin antibody treatment of HFD-fed mice restores the acute effects of leptin to depolarize leptin-receptor-expressing POMC neurons (100 nM, 9/12; change of resting membrane potential,

7.2 ± 0.8 mV, p < 0.01; Figure 5Q). These data illustrate that HFD leads to a blunting of the acute leptin effects in leptin-receptor-expressing POMC neurons, while the neutralizing antibody can restore acute leptin action in leptin-receptor-expressing POMC neurons (Figure 5R). In addition to the enhanced leptin sensitivity evident in the central nervous system (CNS), peripheral tissues also exhibit a higher degree of leptin sensitivity. The mRNA levels of hormone-sensitive lipase (HSL) and the protein levels of p-HSL (but not ATGL) in visceral fat are greatly increased in ALepKO mice, compared to littermate Ctrl mice (Figures S5I–S5K). Taken together, these results further support the hypothesis that partial leptin reduction enhances leptin sensitivity during obesity.

DISCUSSION

We take advantage of our recently developed genetic models of inducible gene elimination in the adult setting to examine leptin action in the context of an otherwise unchanged adipocyte. We wish to emphasize that the initial manipulation of leptin leaves all other adipocyte-derived factors unaltered, at least at the early stages of the process. In other words, in contrast to conventional methods that involve severe weight loss or massive weight gain to alter leptin levels, we describe here a downward titration of leptin levels at the level of the adult mouse, effectively reducing bioavailable leptin concentrations that reach the hypothalamus. We are doing this *without* initially affecting the adipocyte in any other way. This novel experimental paradigm has in fact not been pursued previously and, as such, has allowed us to observe unexpected effects that are consistent with an abrupt sensitization to the actions of leptin (Figure 6).

To date, two prevailing models are proposed to explain leptin action in the brain, summarized in a recent review (Flier, 2019). In the first model, adipocyte-produced leptin in circulation is proportionally elevated with increased fat mass and triggers a response in critical hypothalamic neuronal populations, which ultimately prompts a corresponding increase in energy expenditure with a reduction in food intake (Flier, 2019). Overall, this establishes a model of homeostatic control over specific energy reserves and fat mass. An alternative model argues that the primary signal sensed centrally is not an increase in circulating

---

(D) Effects of acute leptin injections on food intake in ALepKO (n = 8) and littermate control mice (n = 9) after overnight fasting.

(E) DAB staining of p-STAT3 after leptin injection in ALepKO and Ctrl mice.

(F) Gene expression of *pomc* in ARH region after neutralizing leptin antibody treatment.

(G) Gene expression of *socs3* in ARH region after neutralizing leptin antibody treatment.

(H) DAB staining of p-STAT3 after leptin injection in neutralizing hLEP3 treated mice.

(I) Effects on food intake in obese WT mice (vehicle [n = 7] versus mLep3 [n = 6]) were chronically treated with control antibodies (mIGG) or a mouse version of the neutralizing leptin antibody (mLep3).

(J–N) Brightfield illumination (J) of a POMC neuron that expresses leptin receptors from POMC-hrGFP::LepR-cre::tdtomato mice; (K) and (L) show the same neuron under FITC (hrGFP, green cell) and Alexa Fluor 594 (tdtomato, red cell) illumination. Complete dialysis of Alexa Fluor 350 from the intracellular pipette is shown in (M) and a merged image of a POMC neuron targeted for electrophysiological recording (N); merged image. Arrow indicates the targeted cell. Scale bar, 50 μm.

(O) Representative electrophysiological trace demonstrating a leptin-receptor-expressing POMC neuron from chow-diet-fed mice is depolarized by leptin (100 nM).

(P) Representative electrophysiological trace demonstrating a leptin-receptor-expressing POMC neuron from HFD fed mice is depolarized by leptin (100 nM).

(Q) Representative electrophysiological trace demonstrating a leptin-receptor-expressing POMC neuron from HFD fed mice, which is injected with neutralizing antibody, is depolarized by leptin (100 nM).

(R) Histogram illustrates the acute effects of leptin (100 nM) on the membrane potential of leptin-receptor-expressing POMC neurons from chow or HFD fed mice with or without antibody injection.

Data are given as mean ± SEM. Error bars indicate SEM. *p < 0.05; **p < 0.01; ***p < 0.001.
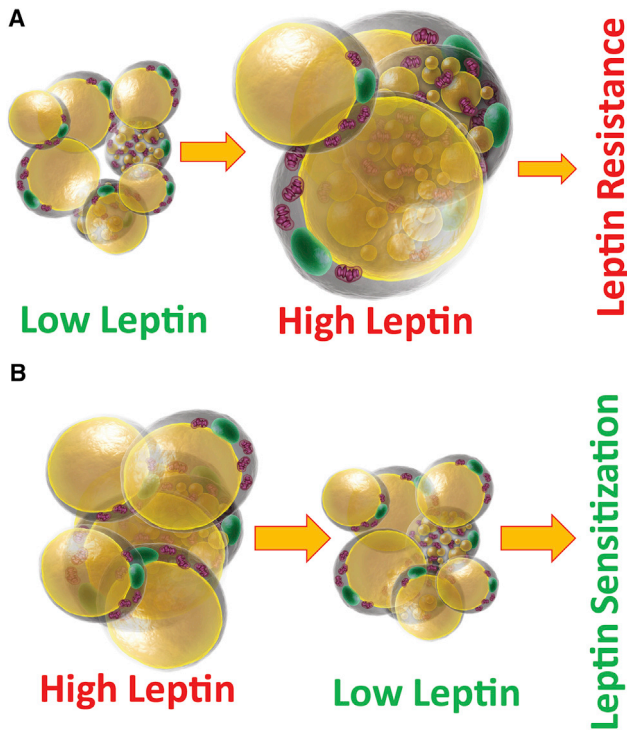
Figure 6. Summary of Relationship of Circulating Leptin Levels and Leptin Sensitivity
(A) With adipose tissue expansion, high leptin levels are achieved in circulation, leading to a high degree of leptin resistance.
(B) Reducing leptin levels in a setting of high circulating leptin restores leptin sensitivity.

leptin levels. Rather, the relevant signal is a *decrease* in circulating leptin levels that signals an energy deficit. This drop in leptin levels leads to an increase in food intake and a reduction in energy expenditure. In both models, the central sensing mechanism critically relies on changes in circulating leptin concentrations. All of the leptin action relies on the presence of functional leptin receptors in the brain and peripheral tissues (Clément et al., 1998). Reducing or eliminating leptin receptor activity by genetic mutation or with a pharmacological receptor antagonist leads to severe obesity in mice. In the obese setting, a leptin receptor antagonist can still produce increased body weight gain and food intake. This leads to the conclusion that diet-induced obese mice retain near maximum endogenous leptin action, but there is still room for further metabolic deterioration by elimination receptor action altogether (Ottaway et al., 2015). However, a recent report indicates that central inhibition of leptin receptor in diet-induced obese mice improves glucose tolerance and hepatic insulin sensitivity (Balland et al., 2019a), which is consistent with our current partial leptin reduction strategy. Further studies indicate that leptin signaling in the arcuate nucleus (ARH) of the hypothalamus of obese mice not only remains functional, but is permanently activated (Balland et al., 2019b). As a result of this persistent activation due to endogenous high circulating leptin concentrations, there is a saturation of leptin signaling with a failure to further respond to even higher concentrations of exogenous leptin. The lack of anorexic effects in the

presence of persistent leptin signaling in the ARH is due to the existence of a potent feedback mechanism that relies on inducing the suppressor of cytokine signaling 3 (SOCS3) and protein tyrosine phosphatase (PTP1B) expression, resulting in a blocked leptin signaling cascade. Of special interest, SOCS3 expression in the ARH area is leptin dependent: higher leptin induces higher SOCS3 expression (Bjørbaek et al., 1998). Our results indicate that partial leptin reduction via genetic manipulation or with leptin neutralizing antibodies reduces SOCS3 expression. Furthermore, PTP1B exerts its inhibitory effect on both leptin and insulin signaling pathways to promote obesity and type 2 diabetes. Thus, in the context of obesity, the major cause of the impaired leptin action may not be the defect in leptin signaling per se but rather the potent feedback mechanisms induced by constitutive activation of leptin signaling that also feeds back on insulin signaling. Partial reduction of leptin action in the ARH ameliorates these feedback mechanisms of leptin signaling and restores both leptin and insulin sensitivity. This may very well be true in other areas of the brain and in the periphery, leading to the potent insulin sensitizing effects that we observe system-wide.

In the context of obesity, hyperleptinemia (Knight et al., 2010), excess circulating lipids (Banks et al., 2004), and inflammation (Myers et al., 2010) are all proposed to be driving forces to induce leptin resistance. However, our data suggest that leptin resistance may primarily stem from high circulating leptin levels, as circulating lipids and inflammation are both shown to stimulate leptin secretion. In clinical studies, a subset of obese individuals has disproportionately low levels of circulating leptin. Accordingly, these obese subjects should retain higher levels of leptin sensitivity and respond favorably to exogenous leptin treatment, as demonstrated by an elegant recent report (Depaoli et al., 2018). Similarly, a partial leptin reduction by weight loss in humans leads to higher leptin sensitivity. In that case, low-dose leptin treatment potentiates the physiological action of leptin, resulting in reversing skeletal muscle, autonomic, and neuroendocrine adaptations (Rosenbaum et al., 2005). Under these conditions, a "low" dose of leptin aimed to restore a physiological leptin level is required to achieve beneficial effects. We suspect that high doses of leptin are unable to exert beneficial effects, since high circulating leptin levels are both necessary and sufficient to induce leptin resistance (Rosenbaum et al., 2005; Scarpace et al., 2005). In addition, individuals on a negative net energy balance, such as during food restriction or a hypocaloric diet, experience weight loss and hence lower leptin levels. It is unclear whether the leptin reduction under such conditions contributes to weight regain or prevents a further weight loss. Some reports indicate that subjects with higher plasma leptin levels at baseline could be more prone to regain lost weight. A greater reduction in leptin levels was better correlated to weight loss maintenance (Crujeiras et al., 2010). Of special importance, a recent study directly examined whether negative energy balance signals could counteract participants' efforts to continue losing weight by increasing food cue reactivity and food intake. They concluded that the reduction in leptin does not counteract weight loss, and it is indeed correlated with further weight loss over the long term (Neseliler et al., 2019). These observations support that the beneficial effects of partial leptin deletion not only occur in rodents, but may also be relevant in humans.

In previous studies, partial leptin deficiency, achieved by the congenital deletion of one copy of the *ob* gene ($ob^{-/+}$ mice) or by the dysregulation of a long noncoding RNA (lncOb) is associated with accelerated weight gain and impaired glucose tolerance (Begriche et al., 2008; Dallner et al., 2019; Farooqi et al., 2001). This is in contrast to our current findings. However, the strategy applied in these studies relies on a *congenital* elimination of *ob* or *lncOb* gene during development rather than the inducible gene deletion at the adult age that we utilize here. The leptin surge during development is crucial for the maturation and function of the neuroendocrine axis (Delahaye et al., 2008). In addition, the actual circulating levels of leptin detected in the adult $ob^{-/+}$ mouse are not decreased, rather increased. Thus, this model cannot be considered to be an effective "partial leptin deficiency model" but rather resembles a model of physiologically increased leptin levels, comparable to what we show in our leptin transgenic mice. In addition, for mice deficient in lncOb, it is still unclear whether the dysregulation of lncOb in mice will affect the expression levels of other genes, as the deletion of lncOb in female mice results in more profound effects in body weight.

Another important concern relates to the effects of leptin on fertility (Barash et al., 1996; Chehab et al., 1996). Complete lack of leptin action triggers infertility since it reflects insufficient fat mass to undergo successful reproduction. There is a legitimate concern that our approach reducing leptin levels may reduce or completely abolish fertility. We tested this in the context of our inducible genetic loss of function model in which we reduced leptin levels by 90% on a HFD, and we observed no impact on fertility at all, with an equal number of pregnancies initiated, with a comparable number of pups with comparable viability.

Based on our observations, we propose that the pharmacological reduction of leptin levels under obese conditions, through the use of neutralizing antibodies, may offer not only a weight loss strategy but, more importantly, confers valuable anti-diabetic properties associated with the ability to titrate down effective leptin concentrations in plasma.

Limitations of Study

We claim beneficial effects of a "partial" reduction of leptin levels in adult mice. A better definition of "partial" is warranted. However, we have to take note that we have demonstrated a very wide therapeutic range for the leptin reduction, with effects leading to leptin sensitization seen anywhere for a 20%–80% reduction in leptin levels. Finally, the dataset presented here has only been validated in rodent models, and we lack any direct proof that the effects will also be seen in non-human primates or in clinical studies. However, the basic adipokine physiology for both leptin and adiponectin has held up extremely well between the rodent and clinical studies. Lastly, we are impressed with the effects obtained on weight but believe that the anti-diabetic actions of leptin neutralization are probably more relevant than the impact on weight loss.

STAR★METHODS

Detailed methods are provided in the online version of this paper and include the following:

- KEY RESOURCES TABLE
- LEAD CONTACT AND MATERIALS AVAILABILITY

- EXPERIMENTAL MODEL AND SUBJECT DETAILS
  - General Mouse Lines
  - ALep-TG Mice
  - Cas9-sgLeptin Mice
  - Alepflox-HZ Mice
  - ALepKO Mice
  - Inducible ob/ob Mice
  - POMC-hrGFP Mice
- METHOD DETAILS
  - Food Intake and Body Weight
  - Glucose and Insulin Tolerance Tests
  - Generation of Human Neutralizing Leptin Antibody
  - ELISA Binding Assay
  - Affinity Measurement with BLI
  - Neutralizing Leptin Antibody Treatment
  - Free Leptin Measurements
  - Metabolic Cage Studies
  - RT-qPCR and Analysis
  - Western Blotting
  - Histology
  - Electrophysiology Studies
- QUANTIFICATION AND STATISTICAL ANALYSIS
- DATA AND CODE AVAILABILITY

AUTHOR CONTRIBUTIONS

S.Z., Y.Z., N.L., Z.Z., Q.Z., Y.D., R.G., C.E.L., and C.M.K. conducted most of the experiments. H.Y. and K.W.W. conducted patch-clamp study and analyzed the results. K.S. generated the Cas9-based mouse model. W.X. produced different versions (in mouse and human chimera and mouse antibodies for *in vitro* and *in vivo* assays). H.D. converted the scFv fragments into full IgGs. M.K. generated TRE-leptin mice. R.D.S. constructed the phage library and isolated the leptin antibodies from the library. G.V.C. and A.K.O. kindly generated and provided the leptin-floxed mice. N.Z., Z.A. R.D.S., W.X., and H.D. generated the leptin antibodies. N.Z. and Z.A. were involved in experimental designs for antibody studies and data interpretation. A.C., J.S., and T.L. helped with MBH isolation and discussion. S.Z. and P.E.S. wrote the manuscript. C.M.K. revised the manuscript. P.E.S. and J.K.E. were involved in experimental design, experiments, data analysis, and the interpretation of data.

REFERENCES

Ahima, R.S., and Flier, J.S. (2000). Leptin. Annu. Rev. Physiol. *62*, 413–437.

Balland, E., Chen, W., Dodd, G.T., Conductier, G., Coppari, R., Tiganis, T., and Cowley, M.A. (2019a). Leptin signaling in the arcuate nucleus reduces insulin's capacity to suppress hepatic glucose production in obese mice. Cell Rep. *26*, 346–355.e3.

Balland, E., Chen, W., Tiganis, T., and Cowley, M.A. (2019b). Persistent leptin signalling in the arcuate nucleus impairs hypothalamic insulin signalling and glucose homeostasis in obese mice. Neuroendocrinology. https://doi.org/10.1159/000500201.

Banks, W.A., Coon, A.B., Robinson, S.M., Moinuddin, A., Shultz, J.M., Nakaoke, R., and Morley, J.E. (2004). Triglycerides induce leptin resistance at the blood-brain barrier. Diabetes *53*, 1253–1260.

Barash, I.A., Cheung, C.C., Weigle, D.S., Ren, H., Kabigting, E.B., Kuijper, J.L., Clifton, D.K., and Steiner, R.A. (1996). Leptin is a metabolic signal to the reproductive system. Endocrinology *137*, 3144–3147.

Begriche, K., Lettéron, P., Abbey-Toby, A., Vadrot, N., Robin, M.A., Bado, A., Pessayre, D., and Fromenty, B. (2008). Partial leptin deficiency favors diet-induced obesity and related metabolic disorders in mice. Am. J. Physiol. Endocrinol. Metab. *294*, E939–E951.

Bjørbaek, C., Elmquist, J.K., Frantz, J.D., Shoelson, S.E., and Flier, J.S. (1998). Identification of SOCS-3 as a potential mediator of central leptin resistance. Mol. Cell *1*, 619–625.

Bouret, S.G., Draper, S.J., and Simerly, R.B. (2004). Trophic action of leptin on hypothalamic neurons that regulate feeding. Science *304*, 108–110.

Chehab, F.F., Lim, M.E., and Lu, R. (1996). Correction of the sterility defect in homozygous obese female mice by treatment with the human recombinant leptin. Nat. Genet. *12*, 318–320.

Clément, K., Vaisse, C., Lahlou, N., Cabrol, S., Pelloux, V., Cassuto, D., Gourmelen, M., Dina, C., Chambaz, J., Lacorte, J.M., et al. (1998). A mutation in the human leptin receptor gene causes obesity and pituitary dysfunction. Nature *392*, 398–401.

Crujeiras, A.B., Goyenechea, E., Abete, I., Lage, M., Carreira, M.C., Martínez, J.A., and Casanueva, F.F. (2010). Weight regain after a diet-induced loss is predicted by higher baseline leptin and lower ghrelin plasma levels. J. Clin. Endocrinol. Metab. *95*, 5037–5044.

Dallner, O.S., Marinis, J.M., Lu, Y.H., Birsoy, K., Werner, E., Fayzikhodjaeva, G., Dill, B.D., Molina, H., Moscati, A., Kutalik, Z., et al. (2019). Dysregulation of a long noncoding RNA reduces leptin leading to a leptin-responsive form of obesity. Nat. Med. *25*, 507–516.

Delahaye, F., Breton, C., Risold, P.Y., Enache, M., Dutriez-Casteloot, I., Laborie, C., Lesage, J., and Vieau, D. (2008). Maternal perinatal undernutrition drastically reduces postnatal leptin surge and affects the development of arcuate nucleus proopiomelanocortin neurons in neonatal male rat pups. Endocrinology *149*, 470–475.

Depaoli, A., Long, A., Fine, G.M., Stewart, M., and O'Rahilly, S. (2018). Efficacy of Metreleptin for weight loss in overweight and obese adults with low leptin levels. Diabetes *67*.

Farooqi, I.S., Jebb, S.A., Langmack, G., Lawrence, E., Cheetham, C.H., Prentice, A.M., Hughes, I.A., McCamish, M.A., and O'Rahilly, S. (1999). Effects of recombinant leptin therapy in a child with congenital leptin deficiency. N. Engl. J. Med. *341*, 879–884.

Farooqi, I.S., Keogh, J.M., Kamath, S., Jones, S., Gibson, W.T., Trussell, R., Jebb, S.A., Lip, G.Y., and O'Rahilly, S. (2001). Partial leptin deficiency and human adiposity. Nature *414*, 34–35.

Flier, J.S. (2019). Starvation in the midst of plenty: reflections on the history and biology of insulin and leptin. Endocr. Rev. *40*, 1–16.

Flier, J.S., and Maratos-Flier, E. (2017). Leptin's physiologic role: does the emperor of energy balance have no clothes? Cell Metab. *26*, 24–26.

Friedman, J. (2016). The long road to leptin. J. Clin. Invest. *126*, 4727–4734.

Friedman, J.M., and Halaas, J.L. (1998). Leptin and the regulation of body weight in mammals. Nature *395*, 763–770.

Fukuda, M., Williams, K.W., Gautron, L., and Elmquist, J.K. (2011). Induction of leptin resistance by activation of cAMP-Epac signaling. Cell Metab. *13*, 331–339.

Halaas, J.L., Boozer, C., Blair-West, J., Fidahusein, N., Denton, D.A., and Friedman, J.M. (1997). Physiological response to long-term peripheral and central leptin infusion in lean and obese mice. Proc. Natl. Acad. Sci. USA *94*, 8878–8883.

Hausman, G.J., Barb, C.R., and Lents, C.A. (2012). Leptin and reproductive function. Biochimie *94*, 2075–2081.

He, Z., Gao, Y., Alhadeff, A.L., Castorena, C.M., Huang, Y., Lieu, L., Afrin, S., Sun, J., Betley, J.N., Guo, H., et al. (2018). Cellular and synaptic reorganization of arcuate NPY/AgRP and POMC neurons after exercise. Mol. Metab. *18*, 107–119.

Knight, Z.A., Hannan, K.S., Greenberg, M.L., and Friedman, J.M. (2010). Hyperleptinemia is required for the development of leptin resistance. PLoS One *5*, e11376.

Koch, C.E., Lowe, C., Pretz, D., Steger, J., Williams, L.M., and Tups, A. (2014). High-fat diet induces leptin resistance in leptin-deficient mice. J. Neuroendocrinol. *26*, 58–67.

Kusminski, C.M., Park, J., and Scherer, P.E. (2014). MitoNEET-mediated effects on browning of white adipose tissue. Nat. Commun. *5*, 3962.

Kusminski, C.M., Bickel, P.E., and Scherer, P.E. (2016). Targeting adipose tissue in the treatment of obesity-associated diabetes. Nat. Rev. Drug Discov. *15*, 639–660.

Mark, A.L. (2013). Selective leptin resistance revisited. Am. J. Physiol. Regul. Integr. Comp. Physiol. *305*, R566–R581.

Montague, C.T., Farooqi, I.S., Whitehead, J.P., Soos, M.A., Rau, H., Wareham, N.J., Sewter, C.P., Digby, J.E., Mohammed, S.N., Hurst, J.A., et al. (1997). Congenital leptin deficiency is associated with severe early-onset obesity in humans. Nature *387*, 903–908.

Myers, M.G., Jr., Leibel, R.L., Seeley, R.J., and Schwartz, M.W. (2010). Obesity and leptin resistance: distinguishing cause from effect. Trends Endocrinol. Metab. *21*, 643–651.

Neseliler, S., Hu, W., Larcher, K., Zacchia, M., Dadar, M., Scala, S.G., Lamarche, M., Zeighami, Y., Stotland, S.C., Larocque, M., et al. (2019). Neurocognitive and hormonal correlates of voluntary weight loss in humans. Cell Metab. *29*, 39–49.e4.

Noh, K., Mangala, L.S., Han, H.D., Zhang, N., Pradeep, S., Wu, S.Y., Ma, S., Mora, E., Rupaimoole, R., Jiang, D., et al. (2017). Differential effects of EGFL6 on tumor versus wound angiogenesis. Cell Rep. *21*, 2785–2795.

Nunziata, A., Funcke, J.B., Borck, G., von Schnurbein, J., Brandt, S., Lennerz, B., Moepps, B., Gierschik, P., Fischer-Posovszky, P., and Wabitsch, M. (2019). Functional and phenotypic characteristics of human leptin receptor mutations. J. Endocr. Soc. *3*, 27–41.

Odle, A.K., Haney, A., Allensworth-James, M., Akhter, N., and Childs, G.V. (2014). Adipocyte versus pituitary leptin in the regulation of pituitary hormones: somatotropes develop normally in the absence of circulating leptin. Endocrinology *155*, 4316–4328.

Ogawa, Y., Masuzaki, H., Ebihara, K., Shintani, M., Aizawa-Abe, M., Miyanaga, F., and Nakao, K. (2002). Pathophysiogical role of leptin in lifestyle-related diseases. Studies with transgenic skinny mice overexpressing leptin. J. Diabetes Complications *16*, 119–122.

Ottaway, N., Mahbod, P., Rivero, B., Norman, L.A., Gertler, A., D'Alessio, D.A., and Perez-Tilve, D. (2015). Diet-induced obese mice retain endogenous leptin action. Cell Metab. *21*, 877–882.

Pinto, S., Roseberry, A.G., Liu, H., Diano, S., Shanabrough, M., Cai, X., Friedman, J.M., and Horvath, T.L. (2004). Rapid rewiring of arcuate nucleus feeding circuits by leptin. Science 304, 110–115.

Rosenbaum, M., Goldsmith, R., Bloomfield, D., Magnano, A., Weimer, L., Heymsfield, S., Gallagher, D., Mayer, L., Murphy, E., and Leibel, R.L. (2005). Low-dose leptin reverses skeletal muscle, autonomic, and neuroendocrine adaptations to maintenance of reduced weight. J. Clin. Invest. 115, 3579–3586.

Scarpace, P.J., Matheny, M., Tümer, N., Cheng, K.Y., and Zhang, Y. (2005). Leptin resistance exacerbates diet-induced obesity and is associated with diminished maximal leptin signalling capacity in rats. Diabetologia 48, 1075–1083.

Scherer, P.E. (2016). The multifaceted roles of adipose tissue-therapeutic targets for diabetes and Beyond: the 2015 Banting lecture. Diabetes 65, 1452–1461.

Shimomura, I., Hammer, R.E., Ikemoto, S., Brown, M.S., and Goldstein, J.L. (1999). Leptin reverses insulin resistance and diabetes mellitus in mice with congenital lipodystrophy. Nature 401, 73–76.

Sun, J., Gao, Y., Yao, T., Huang, Y., He, Z., Kong, X., Yu, K.J., Wang, R.T., Guo, H., Yan, J., et al. (2016). Adiponectin potentiates the acute effects of leptin in arcuate pomc neurons. Mol. Metab. 5, 882–891.

Zelissen, P.M., Stenlof, K., Lean, M.E., Fogteloo, J., Keulen, E.T., Wilding, J., Finer, N., Rössner, S., Lawrence, E., Fletcher, C., et al. (2005). Effect of three treatment schedules of recombinant methionyl human leptin on body weight in obese adults: a randomized, placebo-controlled trial. Diabetes Obes. Metab. 7, 755–761.

Zeltser, L.M. (2015). Developmental influences on circuits programming susceptibility to obesity. Front. Neuroendocrinol. 39, 17–27.

Zhao, S., Mugabo, Y., Iglesias, J., Xie, L., Delghingaro-Augusto, V., Lussier, R., Peyot, M.L., Joly, E., Taïb, B., Davis, M.A., et al. (2014). Alpha/beta-hydrolase domain-6-accessible monoacylglycerol controls glucose-stimulated insulin secretion. Cell Metab. 19, 993–1007.

Zhu, Y., Gao, Y., Tao, C., Shao, M., Zhao, S., Huang, W., Yao, T., Johnson, J.A., Liu, T., Cypess, A.M., et al. (2016). Connexin 43 mediates white adipose tissue Beiging by facilitating the propagation of sympathetic neuronal signals. Cell Metab. 24, 420–433.

Zhu, Y., Zhao, S., Deng, Y., Gordillo, R., Ghaben, A.L., Shao, M., Zhang, F., Xu, P., Li, Y., Cao, H., et al. (2017). Hepatic GALE regulates whole-body glucose homeostasis by modulating Tff3 expression. Diabetes 66, 2789–2799.

STAR★METHODS

KEY RESOURCES TABLE

REAGENT or RESOURCE	SOURCE	IDENTIFIER
Antibodies		
phospho- HSL	Cell Signaling	Cat#.4139; RRID: AB_2135495
Beta-actin	Sigma-Aldrich	Cat#. A4700; RRID: AB_476730
pSTAT3 antibodies	Cell Signaling	Cat#9131; RRID: AB_331586
Cas9	Thermo-fisher	Cat#: PA5-90171; RRID: AB_2805947
Normal Donkey Serum	Jackson ImmunoResearch	RRID: AB_2337258
a biotinylated donkey anti-rabbit antibody	Jackson ImmunoResearch	RRID: AB_2721862
Alexa Fluor350 Hydrazide	Thermo Fisher	Cat# A10439
Goat anti-rabbit IRDye 800CW	Li-Cor	Cat#: 925-32211; RRID: AB_2651127
Donkey anti-mouse IRDye 680RD	Li-Cor	Cat#: 926-68072; RRID: AB_10953628
Chemicals, Peptides, and Recombinant Proteins		
Glucose	GIBCO	Cat#: 15023-021
TRIzol Reagent	Thermo Fisher	Cat# 15596018
Insulin	Eli Lilly	Product ID: A10008415
Recombinant mouse Leptin	National Hormone & Peptide	Lot # AFP 1819
Dulbecco's Phosphate Buffered Saline	Sigma-Aldrich	Cat#: D8537-500ML
Doxycycline Hyclate	Sigma-Aldrich	Cat#: BP780
High Fat Diet (HFD)	Bio-Serv	Cat# S1850
HFD-DOX600	Bio-Serv	Cat# S7060
HFD-DOX10	Bio-Serv	Cat# S7341
Chow diet with DOX 600	Bio-Serv	Cat# S4107
Hydrogen Peroxide	Sigma-Aldrich	Cat# H3410
Sodium hydroxide	Sigma-Aldrich	Cat# S8045
Triton X-100	Sigma-Aldrich	Cat# X100-500ML
Sodium Azide	Sigma-Aldrich	Cat# S2002
DAB Substrate	Sigma-Aldrich	Cat# 11718096001
Chloral Hydrate	Sigma-Aldrich	Ca# 15307
$CaCl_2$	Sigma-Aldrich	Ca# C7902
$MgCl_2$	Fisher Scientific	Cat#: M35-500
HEPES	Gibco	Cat#: 15630-080
Potassium Gluconate	Sigma-Aldrich	Ca# G4500-100G
NaH_2PO_4	Sigma-Aldrich	Ca# 52074
$NaHCO_3$	Sigma-Aldrich	Ca# S5761
EGTA	Sigma-Aldrich	Ca# E3889
Control antibodies	This paper	N/A
ChromPure Guinea Pig IgG, whole molecule	Jackson ImmunoResearch	RRID: AB_2337022
Mouse IgG Control Antibody	Vector Laboratories	Ca# I-2000
Leptin neutralizing antibodies	This paper	N/A
Critical Commercial Assays		
Mouse leptin ELISA kit	Crystal Chem	Cat#: 90030
iScript cDNA synthesis Kit	BIO-RAD	Cat# 170-8891
Sybr Green Master Mix	Thermo Fisher	Cat# A25778
Pierce BCA Protein Assay kit	Thermo Fisher	Cat# 23225
Mouse Ultrasensitive insulin ELISA kit	ALPCO	Cat# 80-INSMSU-E01
Mouse adiponectin ELISA kit	Millipore	Cat#: EZMADP-60K

Continued

REAGENT or RESOURCE	SOURCE	IDENTIFIER
Experimental Models: Organisms/Strains		
Mouse: WT C57BL6 /J	Jackson Laboratory	JAX. 000664
Mouse: transgenic adiponectin-rtTA	Zhu et al., 2017	N/A
Mouse: transgenic Tre-Cre	Jackson Laboratory	JAX 006234
Mouse: transgenic Rosa26-Cas9	Jackson Laboratory	JAX 026179
Mouse: transgenic Tre-Leptin mouse	This paper	N/A
Mouse: transgenic sgLeptin	This paper	N/A
Mouse: Leptin floxed	Odle et al., 2014	N/A
Mouse: POMC-hrGFP mice	Jackson Laboratory	JAX:006421
Mouse: LepR-cre mice	Jackson Laboratory	JAX:008320
Mouse: Tdtomato mice	Jackson Laboratory	JAX:007908
Oligonucleotides		
Primers for qPCR	See Table S1- this paper	N/A
Primers for genotyping	See Table S2- This paper	N/A
Software and Algorithms		
Excel	Microsoft	N/A
Word	Microsoft	N/A
PowerPoint	Microsoft	N/A
Prism	GraphPad Software	GraphPad Software
Illustrator	Adobe	N/A
Other		
Keyence BZ-X700 Fluorescence Microscope	Keyence	N/A
An Axopatch 700B Amplifier	Molecular Devices	N/A
Zeiss Axioskop FS2 Microscope	Zeiss	N/A
Odyssey Infrared Imager	Li-Cor	N/A

LEAD CONTACT AND MATERIALS AVAILABILITY

Further information and requests for resources and reagents should be directly to and will be fulfilled by Philipp Scherer (philipp.scherer@utsouthwestern.edu).

EXPERIMENTAL MODEL AND SUBJECT DETAILS

All animal experimental protocols have been approved by the Institutional Animal Care and Use Committee of University of Texas Southwestern Medical Center at Dallas. All mice (3-5 mice per cage, if not specially indicated) were housed under standard laboratory conditions (12 h on/off; lights on at 7:00 a.m.) and temperature-controlled environment with food and water available ad libitum. Mice were fed a standard chow-diet (number 5058, LabDiet, St. Louis, MO), a Doxycycline (DOX)-chow diet (600 mg/kg Dox; BioServ, Frenchtown, NJ) or HFD with two different Dox concentrations in the diet HFD-DOX10 (10mg/kg Dox) and HFD-DOX600 (600 mg/kg Dox) (Made by BioServ upon special request, Frenchtown, NJ) for various periods as indicated in the figure legends. All experiments were initiated at approximately 7 or 8 weeks of age, unless indicated otherwise. For all of the in vivo experiments, littermate control mice were used. Water and cages were autoclaved. Cages were changed every other week, and the health status of the mice was monitored using the Allentown sentinel filter, which started in the second quarter of 2017. The mouse genotype did not cause visible changes in initial weight, health or immune status. In all of the experiments, only male mice were used, as female mice are resistance to obesity and type 2 diabetes. The age and number of the mice used for the experiments are indicated for each experiments in the figure legends. In order to ensure the reproducibility, two separate cohorts of mice were used. No inclusion or exclusion criteria were used. The experiments were not randomized. No statistical method was used to predetermine the sample size for the animals. All of our experimental animals were kept under barrier conditions under constant veterinary supervision and did not display any signs of distress or pathological changes that warranted veterinary intervention.

As this study involved a large number of different mouse lines, we list the detailed information for all mouse lines with respect to mouse background, breeding strategy and genotyping assays that were used in this study:

General Mouse Lines

Several general mouse lines were utilized to achieve adipocyte-specific overexpression or know down effects. Adiponectin-rtTA (APN-rtTA) mice on the C57BL/6 background were generated as previously described (Zhu et al., 2017). *TRE*-Cre (JAX 006234) and Rosa26-Cas9 (JAX 026179) mice were both on C57BL/6 background and were purchased from The Jackson Laboratory. In the presence of doxycycline, the combined presence of APN-rtTA and TRE-Cre will drive Cre expression specifically in adipocytes in a dose-dependent manner.

ALep-TG Mice

A doxycycline (DOX)-inducible mouse model of leptin (*TRE*-Lep mouse) on the C57/BL6 background was generated by subcloning the mouse *ob* open reading frame into the pTRE vector (Clontech Laboratories) with a rabbit β-globin 3′ untranslated region. For proper founder screening, we have crossed five TRE-leptin positive male mice (generated by the UTSW Transgenic Core) with homozygous APN-rtTA females. Upon one week Doxycycline supplementation in the chow diet, the mice were euthanized and tissue and blood samples were collected. Only lines with higher leptin mRNA in the fat depots but not in other tissues and elevated leptin levels were chosen as a valid founder mice. For the breeding strategy (Figure S1A), TRE-leptin mice were crossed with homozygous APN-rtTA mice to generate ALep-TG mice with both APN-rtTA and TRE-leptin plus littermate control mice, which only express APN-rtTA without transgene expression.

Cas9-sgLeptin Mice

To achieve cell-specific elimination of leptin, we generated a transgenic mouse line with ubiquitously expressed tandem repeats of two small guide RNA (sgRNAs) under the control of the U6 promoter (sgRNA mice). To achieve adipose tissue specificity, we generated a compound transgenic mouse model that combines aforementioned APN-rtTA, TRE-Cre and the Rosa26-flox-stop-flox-cas9 alleles, which enables us to inducibly activate Cas9 activity in the presence of doxycycline, specifically in mature adipocytes, as verified by western blotting of the sWAT (Figure S1C). In combination with the ubiquitously expressed sgRNA transgene, this allows for the doxycycline-inducible elimination of leptin in the adipose tissues of adult mice (the Cas9-sgLeptin mouse). For the breeding strategy (Figure S1B), we crossed APN-rtTA, TRE-Cre and rosa26-Cas9 mice with mice carrying the APN-rtTA and sgLeptin to generate Cas9-sgLeptin mice with expressing all the four transgenes (APN-rtTA, TRE-Cre, Rosa26-Cas9 and sgleptin) and littermate control mice, which express Apn-rtTA, Rosa26-Cas9 and sgleptin without TRE-Cre. All the mice were on a pure C57/BL6 background.

Alepflox-HZ Mice

The leptin floxed mouse (leptin flox/flox) on an FVB.P129 background was generated and kindly provided by Dr. Childs' group. They designed a specific construct that in which exon 3 was floxed in the leptin gene. In the initial study performed, upon crossing floxed leptin mice with APN-Cre mice to obtain adipocyte-specific KO of leptin from the embryonic stage, circulating leptin levels in this mouse were not detectable and the mouse behaves exactly like *ob/ob* mice (Odle et al., 2014). Leptin floxed mice were then backcrossed to C57BL/6 background for 7 generations in our lab. To generate mice with only one copy of leptin deleted (Alepflox-HZ mice), we crossed the APN-rtTA and leptin flox/+ male mice with the mice carrying APN-rtTA and TRE-Cre (Figure S1D). Using this breeding strategy, the mice (Alepflox-HZ) mice have APN-rtTA, TRE-Cre and leptin flox/+, while the littermate controls have APN-rtTA and leptin flox/+ without TRE-Cre. *ob/+* mice are also a similar mouse model that deletes one cope of leptin allele, however, compared to Alep-HZ mice used in this study, *ob/+* mice do not have the capacity to do this inducibly, since the deletion is constitutive. In this study, ALep-HZ mice were induced only at the adult stage, leading to a clearly distinct phenotype from the ob/+ mice.

ALepKO Mice

For the breeding strategy (Figure S1E), we crossed APN-rtTA, TRE-Cre, leptin flox/flox male mice with female mice containing APN-rtTA and leptin flox/flox. The ALepKO mice used in this study contain APN-rtTA, TRE-Cre and the leptin flox/flox locus and the littermate control mice have APN-rtTA and leptin flox/flox without TRE-Cre. After backcrossing leptin floxed mice with C57BL/6 mice for 7 generations, we assumed that all the mice are on a pure C57BL/6 background.

Inducible ob/ob Mice

This mouse model has been used to verify our leptin neutralizing antibody. We used the same breeding strategy as ALepKO mice (Figure S1E). The only difference lies in the timing of the induction of the leptin deletion. Leptin deletion in ALepKO mice was induced at adult age (at least 7-week old), while the inducible ob/ob mice were induced during the embryonic stage (2 weeks after pregnancy). Inducible *ob/ob* mice behave similar but not exactly like real *ob/ob* mice, as in our inducible *ob/ob* mice, a tiny amount of circulating leptin can be detected in plasma. For the genotyping of the control mice, mice have APN-rtTA and leptin flox/flox and do not have TRE-Cre.

POMC-hrGFP Mice

8-10 week old pathogen-free male POMC-hrGFP::LepR-cre::tdtomato(POMC-hrGFP mice RRID: IMSR_JAX:006421; LepR-cre mice RRID: IMSR_JAX:008320; Tdtomato mice RRID: IMSR_JAX:007908) on C57BL/6 background were used for electrophysiology Studies. For all the mouse studies, littermate controls were used.

METHOD DETAILS

Food Intake and Body Weight

In order to measure food intake and body weight gain, the mice with different genotyping were single housed. Before each experiment, the mice were acclimated in the single cage for at least one week to reduce the anxiety effects. For some of the studies, the food intake and body weight were measured on a daily basis, while in some chronic studies, these parameters were measured in a weekly basis, as indicated in the figure legends.

For leptin-induced food intake measurements, the mice were starved overnight, and the next day, the mice were received 1μg/kg body weight of leptin at a dose of 10 μl per gram body weight, and then food intake was taken at various time points as indicated in the figure legends.

Instead of using Doxycycline supplementation in the chow or high fat diet to induce gene deletion, we also used oral gavage to deliver Doxycycline in one set of experiments. These experiments were used to confirm the food intake phenotype with the same amount of Doxycycline consumption. The ALepKO and littermate control mice were gavaged orally with 5mg/kg body weight (This dose is calculated based on daily food intake with 10mg doxycycline in HFD). Food take and body weights were measured on a daily basis.

Glucose and Insulin Tolerance Tests

Glucose tolerance tests (GTT) and insulin tolerance tests (ITT) were performed as previously described (Zhao et al., 2014). In brief, for GTT, mice were fasted 4-6 hr in the morning, and the mice were received 2g glucose per kg body weight at the volume calculated based on 10ul/g body weight and blood glucose was measured by glucose meter as indicated time points, shown in different figures; For ITT, 4-6 h fasted mice were injected with a dose of 0.5U insulin per kg body weight, and blood glucose was measured by glucose meter at the indicated time points; For each experiment, area under or above curve (AUC or AAC) was calculated. Insulin and leptin were measured by ELISA kit from Crystal Chem, while adiponectin was measured by ELISA kit (Invitrogen).

Generation of Human Neutralizing Leptin Antibody

A panel of human monoclonal antibodies (mAbs) that bind to human leptin were generated by panning a large diversity human scFv phage displayed antibody library. The scFv hits were converted to full human IgG heavy and light chain constructs, which were co-transfected into human embryonic kidney freestyle 293 (HEK293F) cells using transfection reagent PEI (Sigma). After 7 days of expression, supernatants were harvested and antibodies were purified by affinity chromatography using protein A resin (Repligen) as we reported previously (Noh et al., 2017) for in vitro and in vivo studies. Neutralizing activity of the leptin-binding IgGs were screened *in vitro* with the hypothalamic cell line N2A, which was either treated with a non-immune antibody preparation, pre-incubated with leptin, or with leptin pretreated with an anti-leptin antibody preparation. Three lead anti-leptin antibodies with neutralizing activities (hAbs 2, 3 and 5) were tested in vivo.

ELISA Binding Assay

Corning 96-well EIA/RIA plates were coated overnight at 4°C with leptin recombinant proteins (1 μg/mL) and blocked for 2 hrs at 37°C with 5% non-fat milk. After washing with PBST 3 times, 100 μL of serial diluted anti-LILRB4 antibodies were added and incubated for 45 min at 37°C. Subsequently, the plates were washed with PBST and incubated for 30 min with anti-rabbit or anti-human F(ab')2 HRP-conjugated antibody (Jackson ImmunoResearch Laboratories). The immunoreactions were developed with TMB substrates (Sigma) and stopped by the addition of 2 M sulfuric acid before the plate was read at 450 nm.

Affinity Measurement with BLI

For antibody affinity measurement, antibody (30 μg/mL) was loaded onto the protein G biosensors for 4 min. Following a short baseline in kinetics buffer, the loaded biosensors were exposed to a series of recombinant LILRB4 concentrations (0.1-200 nM) and background subtraction was used to correct for sensor drifting. All experiments were performed with shaking at 1,000 rpm. Background wavelength shifts were measured from reference biosensors that were loaded only with antibody. ForteBio's data analysis software was used to fit the data to a 1:1 binding model to extract an association rate.

Neutralizing Leptin Antibody Treatment

Wild-type (WT) were fed with HFD for 12 weeks to become obese (body weight approximately 50g). As not all the mice response equally to HFD, we chose the mice with equal body weight and similar circulating leptin level for this study. In order to reduce the anxiety effects, each single-housed mouse received PBS injection for one week. Then the mice were grouped and either received leptin neutralizing antibody or vehicle (in the initial screening experiments, PBS was used as vehicle, while in the phenotyping and metabolic cage studies, mouse or human IGG was used as a control antibody. In addition, in one verification experiment, an isotope control antibody, a human IgG1 monoclonal antibody that we identified in house against human cytomegalovirus (hCMV virus), was used as a control antibody) for another two weeks. The mice were i.p. injected twice per week (Tuesdays and Fridays) and food intake and body weight were monitored per injection time. After two weeks' antibody injection, the mice were performed OGTT, and then the mice were euthanized for tissue collection.

For chronic leptin neutralizing antibody treatment, HFD-fed obese mice (around 50g) were single housed, and first treated with PBS injection for one week. Then the mice were either received vehicle (mouse IGG) or mouse version of leptin neutralizing antibody at a dose of 5mg/kg body weight for 6-week period. Body weight and food intake were measured before each injection.

For experiments conducted in thermoneutral conditions, single-housed mice were acclimated in the thermal chamber for two weeks before experiments. Before the antibody treatment, the mice were subjected to an OGTT. Then the mice were injected with PBS for one week, followed by two weeks of leptin neutralizing antibody or human IGG treatment at a dose of 5mg/kg body weight. After two weeks of treatment, the mice were subjected to another OGTT to assess the effects of the leptin neutralizing antibodies.

Free Leptin Measurements

After neutralizing antibody treatment, some leptin in circulation is associated with leptin neutralizing antibody. In order to differentiate free leptin from leptin associated with antibodies, we precipitated 100μl of mouse plasma with anti-mouse IGG beads and centrifuged to isolate the pellet. The supernatant was used for leptin measurements. In this manner, the leptin measured is regarded as free leptin.

Metabolic Cage Studies

We performed various metabolic cage studies on ALepKO and leptin neutralizing antibody-treated HFD-fed mice. In general, all the mice are acclimated in the metabolic cage for one week before measurement. Then the mice were recorded for at least three more days to measure food intake, body weight, locomotor activity, O_2 and CO_2 consumption. Based on O_2 and CO_2, RER and heat production was calculated.

To assess the acute effect of leptin neutralizing antibody in metabolic cage, only body weight and circulating leptin level-matched HFD-fed WT animals were chosen for the experiments. During acclimation period, the mice was received PBS injection every two days to reduce acute injection-induced anxiety effect. Just before the recording, the mice received either human IGG or hLep3 at a dose of 5mg/kg body weight, and then were monitored in the metabolic cages for three more days.

RT-qPCR and Analysis

RNA was extracted from fresh or frozen tissues by homogenization in TRIzol Reagent as previously described (Zhu et al., 2017). We used 0.5 μg RNA to transcribe cDNA with a reverse transcription kit (Bio-Rad). Most of RT-qPCR primers were from Harvard PrimerBank (https://pga.mgh.harvard.edu/primerbank/). The relative expression levels were calculated using the comparative threshold cycle method, normalized to the housekeeping gene *Rps16*.

Western Blotting

Protein extractions were done as previously described. Primary antibodies phospho- HSL (catalog no.4139; Cell Signaling Technology), tubulin (catalog no. sc-53030; Santa Cruz Biotechnology), and actin (catalog no. A4700; Sigma-Aldrich) were used at 1:1,000 dilutions and detected using a secondary immunoglobulin G labeled with infrared dyes emitting at 680 nm (catalog no. 926-68070 and 926-68076; LI-COR Bioscience) or 800 nm (catalog no. 926-32211; LI-COR Bioscience) (both at 1:10,000 dilutions) and then visualized on a LI-COR Odyssey infrared scanner (LI-COR Bioscience). The scanned data were analyzed using Odyssey version 3.0 software (LI-COR Bioscience).

Histology

Adipose tissues and livers were excised and fixed overnight in 10% PBS-buffered formalin and were thereafter switched to 50% ethanol for long time storage. Tissues were processed at the UTSW Molecular Pathology Core. p-STAT3 staining in the brain was previous described (Fukuda et al., 2011). Briefly, overnight fasted mice were injected with leptin at dose of 2.5mg/kg body weight. After 45mins, the mice were heart-perfused and brains were removed. Then the brains were sliced at 5 μm per slide, and the slices were rinsed 3 times for 5 minutes each in PBS, pH 7.4 and then for 20 minutes in 1.0% hydrogen peroxide and 1% Sodium hydroxide in PBS to quench endogenous peroxidase activity. Following a series of PBS washes, slices was incubated for 48-72 hours at 4°C in pSTAT3 antibodies (Cell Signaling Technology) diluted to 1:3,000 in 3% normal donkey serum (Jackson ImmunoResearch Laboratories, West Grove, PA) with 0.25% Triton X-100 in PBS (PBT) with 0.02% sodium azide. After washing in PBS, slices were incubated in a biotinylated donkey anti-rabbit antibody (Jackson ImmunoResearch Laboratories) diluted to 1:1,000 in 3% donkey serum in PBST for 1 hour at room temperature. Tissues were then rinsed in PBS and incubated in ABC (Vectastain Elite ABC kit; Vector Labs, Burlingame, CA) diluted 1:500 in PBS for 1 hour. Slices were washed in PBS then reacted in 0.04% DAB (Sigma, St. Louis, MO) and 0.01% hydrogen peroxide dissolved in PBS.

Electrophysiology Studies

Brain slices were prepared from young adult male mice (8-10 weeks old) as previously described (He et al., 2018). Briefly, male mice were deeply anesthetized with i.p. injection of 7% chloral hydrate and transcardially perfused with a modified ice-cold artificial CSF (ACSF) (described below). The mice were then decapitated, and the entire brain was removed and immediately submerged in ice-cold, carbogen-saturated (95% O_2 and 5% CO_2) ACSF (126 mM NaCl, 2.8 mM KCl, 1.2 mM $MgCl_2$, 2.5 mM $CaCl_2$, 1.25 mM NaH_2PO_4, 26 mM $NaHCO_3$, and 5 mM glucose). Coronal sections (250 μm) were cut with a Leica VT1000S Vibratome

and then incubated in oxygenated ACSF at room temperature for at least 1 h before recording. The slices were bathed in oxygenated ACSF (32°C–34°C) at a flow rate of ∼2 ml/min.

The pipette solution for whole-cell recording was modified to include an intracellular dye (Alexa Fluor350 hydrazide dye) for whole-cell recording: 120 mM K-gluconate, 10 mM KCl, 10 mM HEPES, 5 mM EGTA, 1 mM $CaCl_2$, 1 mM $MgCl_2$, and 2 mM MgATP, 0.03 mM Alexa Fluor 350 hydrazide dye (pH 7.3). Epifluorescence was briefly used to target fluorescent cells, at which time the light source was switched to infrared differential interference contrast imaging to obtain the whole-cell recording (Zeiss Axioskop FS2 Plus equipped with a fixed stage and a QuantEM:512SC electron-multiplying charge-coupled device camera). Electrophysiological signals were recorded using an Axopatch 700B amplifier (Molecular Devices), low-pass filtered at 2–5 kHz, and analyzed offline on a PC with pCLAMP programs (Molecular Devices). Membrane potential was measured by whole-cell current clamp recordings from POMC neurons in brain slices. Recording electrodes had resistances of 2.5–5 MΩ when filled with the K-gluconate internal solution.

Leptin (100nM) was added to the ACSF for specific experiments. Solutions containing drug were typically perfused for 5 min. A drug effect was required to be associated temporally with peptide application, and the response had to be stable within a few minutes. A neuron was considered depolarized or hyperpolarized if a change in membrane potential was at least 2 mV in amplitude.

QUANTIFICATION AND STATISTICAL ANALYSIS

No statistical method was used to predetermine sample size. The experiments were not blind. All statistics were done using Graph-Pad Prism version 7.01. Unpaired Student's t-test was done to compare only two groups. One way or two-way ANOVA was used for comparisons of more than two groups. All values were expressed as the mean ± SEM. In each experiment, n defines the number of mice included, except for patch-clamp study, where n represents the number of cells. $P \leq 0.05$ is regarded as statistically significant.

DATA AND CODE AVAILABILITY

This study did not generate new datasets or codes.